BER and PAPR Reduction of IEEE 802.11a Using RS Coding and SLM Technique

A thesis submitted in partial fulfillment of the

requirements for the award of the Degree of

MASTER of ENGINEERING

in

ELECTRONICS AND COMMUNICATION ENGINEERING

Submitted by:

Vikash Singh
Roll No. 800861029

Under the guidance of:

Dr. KULBIR SINGH
Assistant Professor, ECED

DEPARTMENT OF ELECTRONICS AND COMMUNICATION ENGINEERING

THAPAR UNIVERSITY

PATIALA-147004, Punjab, INDIA.

June 2010

CERTIFICATE

I hereby certify that the work which is being presented in this thesis entitled, **" BER and PAPR Reduction of IEEE 802.11a Using RS Coding and SLM Technique,"** in partial fulfillment of requirements for the award of degree of Master of Engineering in Electronics and Communication from Thapar University, Patiala, is an authentic record of my own work carried under the supervision of Dr. Kulbir Singh.

The matter presented in this thesis has not been submitted in any other University or Institute for the award of Master of Engineering.

(Vikash Singh)

Roll no. 800861029

This is to certify that the above statement made by the candidate is correct and true to the best of my knowledge.

(Dr. Kulbir Singh)

Assistant Professor

ECED, T.U, Patiala-147004, (Punjab)

Dr. A.K. Chatterjee 7.10.

Professor & Head of Department

ECED, T.U, Patiala-147004, (Punjab)

Dr. R.K. Sharma 12.7.10

Dean of Academic Affairs

T.U, Patiala-147004, (Punjab)

ACKNOWLEDGEMENT

I am thankful to my guide Dr. Kulbir Singh, Assistant Professor, Electronics and Communication Engineering Department, Thapar University, Patiala, for his advice, motivation, guidance, moral support, efforts and the attitude with which he solved all of my queries in making this report possible. It has been a great honour to work under him.

I am also thankful to Dr. A.K. Chatterjee, Professor and Head, Electronics and Communication Engineering Department, Thapar University, Patiala, for providing us with adequate infrastructure in carrying the work.

I am also thankful to Mrs. Alpana Agarwal, PG Coordinator, Electronics and Communication Engineering Department, for the motivation and inspiration that triggered me for my work.

I would also like to thank all the faculty members and my friends who were always there at the need of the hour and provided with all the help and facilities, which I required for the completion of my report.

I am also thankful to the authors whose works I have consulted and quoted in this work.

Vikash Singh

Roll No. 800861029

TABLE OF CONTENTS

ABBREVIATIONS

A:

ACI:	Adjacent Channel Interference
AIEE:	American Institute of Electrical Engineers
AWGN:	Additive White Gaussian Noise

B:

BER:	Bit Error Rate
BPSK:	Binary Phase Shift Keying

C:

CP:	Cyclic Prefix
CC:	Convolution Code
CPU:	Centre Processing Unit
CCK:	Complementary Code Keying
CDF:	Cumulative Distribution Function

D:

DSSS:	Direst Sequence Spread Spectrum.
DFT:	Discrete Fourier Transform

F:

FFT:	Inverse Fast Fourier Transform
FHSS:	Frequency Hopping Spread Spectrum
FEC:	Forward Error Correction Code

G:

GI:	Guard interval
GF:	Gloss Field

I:

IRE:	Institute of Radio Engineers
IEEE:	Institute of Electronic and Electrical Engineering
ISM:	Industrial, Scientific and Medical Radio bands
IFFT:	Inverse Fast Fourier Transform
ICI:	Inter channel Interference
ISI:	Inter Symbol Interference

IDFT: Inverse Discrete Fourier Transform

L:

LOS: Line Of Sight

M:

MATLAB: Matrix Laboratory

MBWA: Mobile Broadband Wireless Access

MAC: Multiple Access Control

O:

OFDM: Orthogonal Frequency Division Multiplexing

P:

PA: Power Amplifier

PAPR: Peak to Average Power Ratio

PC: Personal Computer

P/S: Parallel to Serial

PHY: Physical Layer

PDF: Probability Distribution Function

Q:

QPSK: Quadrature Amplitude Modulation

QAM: Quadrature Amplitude Modulation

R:

RS: Reed Solomon

RAM: Random Access Memory

RF: Radio Frequency

RMS: Root Mean Square

S:

SLM: Selective Mapping

SNR: Signal to Noise Ratio

S/P: Serial to Parallel

SCs: Subcarriers

T:

TDMA: Time Division Multiple Access.

TGs: Task Group

W:

WLAN: Wireless Local Area Network

Wi-Fi: Wireless Fidelity

WGs: Working Group

WPAN: Wireless Personal Area Network

WMAN: Wireless Metropolitan Area Network

WRAN: Wireless Regional Area Network

X:

XOR: Exclusive OR

LIST OF FIGURES

LIST OF TABLES

CHAPTER 1
INTRODUCTION

In the recent year, the word PORTABLE is the most common word in today's life. Everyone needs everything should be portable. Wired communication networks can provide the connectivity and performance but not mobility. WLAN provides the solution for portability with connection and performance. Institute of Electrical and Electronics Engineers (IEEE) is the foundation of WLAN product implemented IEEE standard 802.11 in 1997. IEEE 802.11's family has become very popular in every different environment due to their simplicity, low cost, easy installation, location freedom and high data rate. It provides easy way to configuration of computer network using without complex wiring infrastructure. WLAN deals with local area networking where the communication done over the air between the connected devices those are within the range. There is a famous saying "Nothing is constant but change", likewise, every days demands in high speed and data rate produce some technical demands one of them is the demand of high date rates that's why multi carrier transmission has been implemented in IEEE 802.11's family. The IEEE 802.11 standard defines both a Multiple Access Control (MAC) protocol and physical layer implementations at MAC layer; IEEE 802.11 supports both infrastructure and adhoc networks [1].

Orthogonal Frequency Division Multiplexing (OFDM) is a special form of multicarrier transmission, where a single data stream is transmitted over a number of lower rate subcarriers (SCs). It is either a modulation or multiplexing technique because OFDM is to raise robustness against frequency selection fading or narrowband interference. In a single carrier system, fading or interference can cause the entire link to fail, but in a multicarrier system only a small percentage of the SCs will be affected [2]. Today's 802.11 family is divided into many substandard. This thesis is focused on performance analysis of 802.11a

1.1 Background

In 1963 the "American Institute of Electrical Engineers (AIEE)" and the "Institute of Radio Engineers (IRE)" merges together now it's called the "Institute of Electrical

and Electronics Engineers (IEEE)". Today, the IEEE is leading authority for every field such as aerospace, computers, telecommunication, biomedical engineering, electrical power and much more. IEEE is playing a very vital role not only in industry field but also in education field. More than 1430 student branches at colleges and universities in 80 countries prove IEEE's presence in the research community. [3]

Currently there are 22 working Group (WGs) in IEEE 802 and each and every WGs can be divided into subgroup these subgroup are referred to as Task Group (TGs).The most popular WGs are following:

- 802.0, wireless Coordination Active Group
- 802.1, Higher Layer Local Area Network(LAN)Protocols
- 802.3, Ethernet
- 802.11, Wireless Local Area Network (WLAN)
- 802.15, Wireless Personal Area Network (WPAN)
- 802.16, Wireless Metropolitan Area Network (WMAN)
- 802.17, Resilent Packet Ring
- 802.20, Mobile Broadband Wireless Access (MBWA)
- 802.22, Wireless Regional Area Network (WRAN)

1.2 IEEE 802.11 Wireless Local Area Network

In 1997 IEEE implemented 802.11 Wireless LAN standards. IEEE 802.11's family has become very popular in every different environment due to their simplicity, low cost, easy installation, location freedom and high data rate. It provides easy way to configuration of computer network using without wiring complexity.

IEEE 802.11 standard defined that WLANs can be implemented either optical or radio technologies for the transmission of the signals through the air. Firstly the original standard defined rates of 1 Mbps and 2 Mbps. The radio technology is used in WLANs known as Spread Spectrum modulation. Basically there are two types of spread spectrum modulation techniques which are: Frequency Hopping Spread Spectrum (FHSS) and Direst Sequence Spread Spectrum (DSSS) [4]. The main issue of 802.11 was slow data rate mostly in business environment. The later revision of 802.11 can be more classified into three categories.

- IEEE 802.11a
- IEEE 802.11b
- IEEE 802.11g

1.2.1 IEEE 802.11a

IEEE standard 802.11a has been approved in July 1999 include with a new specification. It operates in the 5 GHz spectrum. The IEEE 802.11a standard was designed for better scalability and higher bandwidth application rather than IEEE 802.11b include with the data rates of 6, 9, 12, 18, 24, 36, 48, 54 Mbps using orthogonal frequency division multiplexing (OFDM) modulation. [5]

1.2.2 IEEE 802.11b

IEEE 802.11b extends the original IEEE 802.11 direct sequence spread spectrum (DSSS) standard to operate up to 11 Mbps in the 2.4 GHz unlicensed spectrum using complementary code keying (CCK) modulation. The four data rates of 1, 2, 5.5, and 11 Mbps are specified on up to three non- overlapping channels and the lowest two rates are also allowed on up to 13 overlapping channels. [6]

1.2.3 IEEE802.11 g

The IEEE's 802.11g standard has been ratified in June 2003. The IEEE 802.11g standard provides optional higher-bandwidth up to 54 Mbps. IEEE 802.11g used two technology DSSS and OFDM at the 2.4 GHz ISM band. [7]

1.3 Why 802.11a

As the number of WLAN user increases, so does the number of hotspots. The need of high bandwidth on short distances emerges. Bandwidth requirements can be satisfied by using the IEEE 802.11a based WLAN [5]. This standard provides higher throughput on satisfactory distances using 5 GHz frequency band [8]. This band has up to 24 non-overlapping channels (depending on the country’s spectrum regulative) compared to 3 such channels in 2.4 GHz band. Hence IEEE 802.11a should suffer less Co-Channel Interference, compared to its concurrent system [9]. The IEEE 802.11a standard uses the 5-GHz range, which is not as interference-prone (compared to the

2.4-GHz band), due to the relatively minimal technologies operating in this domain. [10]

1.4 Objective of Thesis

The objectives of thesis are

- To analyse the BER performance of 802.11a over different channel condition, AWGN, Ricean fading, Rayleigh fading and Nakagami fading channel.
- To analyse the BER performance of 802.11a for different Doppler shifts, delay spread and CP.
- To analyse the BER performance of 802.11a using different FEC.
- To analyse the PAPR for IEEE 802.11a and improve it with SLM technique.

1.5 Organization of Thesis

The thesis has been organized in the following chapters.

Chapter 2: This chapter gives an overview of OFDM, advantages & drawbacks of OFDM transmission, PAPR & effects of PAPR on OFDM Signals, and SLM technique.

Chapter 3: This chapter discusses IEEE 802.11a Physical Layer Model.

Chapter 4: Different channel impairments and models are discussed.

Chapter 5: This chapter provides the simulation results and comparisons.

Chapter 6: Discuss the important conclusion of the thesis.

CHAPTER 2

OFDM

OFDM is a special form of multicarrier modulation (MCM), where a single data stream is transmitted over a number of lower rate subcarriers. It is worth mentioning here that OFDM can be seen as either a modulation technique or a multiplexing technique. One of the main reasons to use OFDM is to increase the robustness against frequency selective fading and narrowband interference. In a single carrier system, a single fade or interferer can cause the entire link to fail, but in a multicarrier system, only a small percentage of subcarriers will be affected. Error correction coding can then be used to correct the few erroneous subcarriers.

2.1 Fundamentals of OFDM Transmission

OFDM is a technique for transmitting data in parallel by using a large number of modulated sub-carriers. In an OFDM signal, a higher bit rate channel is divided into multiple orthogonal sub-channels in the frequency domain with lower bit rates. The orthogonality of the carriers means that each carrier has an integer number of cycles over a symbol period. Due to this, the spectrum of each carrier has a null at the centre frequency of each of the other carriers in the system. This results in no interference between the carriers, although their spectra overlap. The separation between carriers is theoretically minimal so there would be a very compact spectral utilization [10].

OFDM systems are attractive for the way they handle ISI (inter symbol interference), which is usually introduced by frequency selective multipath fading in a wireless environment. Each sub-carrier is modulated at a very low symbol rate, making the symbols much longer than the channel impulse response. In this way, ISI is diminished. Moreover, if a guard interval between consecutive OFDM symbols is inserted, the effects of ISI can completely vanish. This guard interval must be longer than the multipath delay. Although each sub-carrier operates at a low data rate, a total high data rate can be achieved by using a large number of sub-carriers. ISI has very small or no effect on the OFDM systems hence an equalizer is not needed at the receiver side. A more complete description of an OFDM signal can be seen in fig. 2.1, which shows, an OFDM signal is divided in both time and frequency domain and so

increases the capacity of the system in addition to the less interference of the adjacent symbols

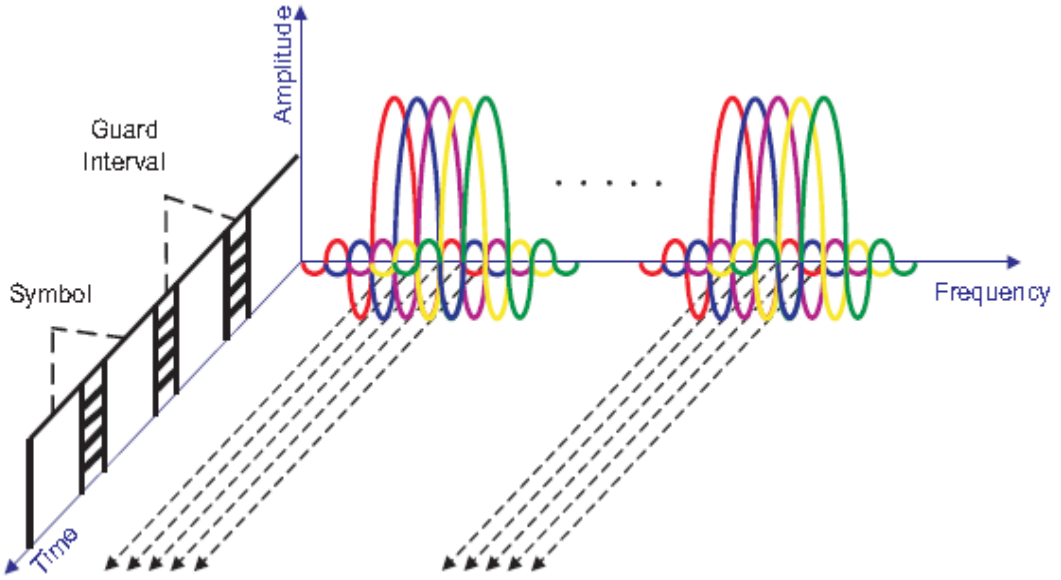

Figure 2.1: OFDM time/frequency representation [11]

2.1.1 Mathematical Representation of OFDM

The mathematical representation of OFDM is described below. Consider a data sequence $(b_0, b_1, \dots, b_{n-1})$, where each b_n is complex number $d_n = a_n + jb_n$. The result of DFT operation on the vector $\{2d_n\}_{n=0}^{N-1}$ is then the vector $S = (S_0, S_1, \dots, S_{n-1})$ of N complex numbers with

$$S_n = \sum_{n=0}^{N-1} 2d_n e^{-j\left(\frac{2\pi n}{N}\right)} = 2\sum_{n=0}^{N-1} 2d_n e^{-j\left(\frac{2\pi f_n t_n}{N}\right)}, \qquad m = 0,1, \dots N-1 \qquad (2.1)$$

where

$$f_n \triangleq {}^{n}/_{n\Delta t} \qquad (2.2)$$

$$t_m \triangleq m\Delta t \qquad (2.3)$$

and Δt is an arbitrarily chosen interval. The real part of S has components

$$Y_m = 2\sum_{n=0}^{N-1} (a_n \cos 2\pi f_n t_m + b_n sin 2\pi f_n t_m), m = 0,1, \dots N-1 \qquad (2.4)$$

if these components are applied to a low pass filter at time intervals Δt, a signal is obtained, which closely approximates the frequency division multiplexed signal as

$$y(t) = 2 \sum_{n=0}^{N-1} (a_n cos2\pi f_n t + b_n sin2\pi f_n t) , 0 \leq t \leq N\Delta t \qquad (2.5)$$

in order to recover the modulated data, a DFT with twice the sampling rate is employed. This is necessary since only the real part of the modulated signal in transmitted. Therefore, the DFT operates on 2N samples

$$Y_m = y\left(k\frac{\Delta t}{2}\right) \qquad (2.6)$$

$$Y_m = 2 \sum_{n=0}^{N-1} (a_n \cos 2\pi nk/2N + b_n sin2\pi nk/2N), \quad k = 0,1, \dots ,2N - 1 \qquad (2.7)$$

the result of the DFT operation is then

$$x_l = \frac{1}{2} \sum_{k=0}^{2N-1} Y_k \, e^{-j\left(\frac{2\pi lk}{2N}\right)}, \begin{cases} 2a_0, & l = 0 \\ a_l - jb_l, l = 1,2, \dots , N - 1 \\ irrelevent, l > N - 1 \end{cases} \qquad (2.8)$$

the original data $a_1$and b_1 can then be extracted as the real and imaginary part of x_l (except at l=0)[7]. Since the sinusoidal components of the parallel input are time limited, they have a $\left[\frac{sinf}{f}\right]^2$ shaped power spectrum. This special shape ensures that as long as the components are samples at the right instance, the neighbouring components have zero contribution. This orthogonal nature of the OFDM symbols helps prevent ICI. [2]

2.1.2 IFFT and FFT Implementation

Inverse DFT and DFT are critical in the implementation of an OFDM system.

$$IDFT\, x(n) = \frac{1}{N} \sum_{k=0}^{N-1} X(k) \, e^{j\frac{2\pi}{N}kn} \qquad (2.9)$$

$$DFT\ X(k) = \sum_{k=0}^{N-1} x(n)\, e^{-j\frac{2\pi}{N}kn} \tag{2.10}$$

IFFT and FFT algorithms are the fast implementation for the IDFT and DFT. Let $\{X_k\}_{k=0}^{N-1}$ be the complex symbols to be transmitted by OFDM modulation of the OFDM signal can be expressed as

$$x(t) = \sum_{k=0}^{N-1} X_k\, e^{j2\pi f_k t} = \sum_{k=0}^{N-1} X_k\, \psi_k(t)\ , for\ 0 \le t \le T_s \tag{2.11}$$

where $f_k = f_k + k\,\Delta f$

and

$$\varphi_k(t) = \begin{cases} e^{j2\pi f_k}, if\ \ 0 \le t \le T_s \\ 0 \quad\quad , otherwise \end{cases} \tag{2.12}$$

for $k = 0,1, \dots, N-1$, T_s and Δf are called the symbol duration and subchannel space of OFDM, respectively. In order for receiver to demodulate OFDM signal, the symbol duration must be long enough such that T_s Δf=1, which is also called orthogonality condition. Because of the orthogonality condition, we have

$$= \frac{1}{T_s}\int_0^{T_s} \psi_k\,(t)\,\psi_l^*\ dt$$

$$= \frac{1}{T_s}\int_0^{T_s} e^{j2\pi(f_k - f_l)\,t}\,dt$$

$$= \frac{1}{T_s}\int_0^{T_s} e^{j2\pi(K-l)\,t}\,dt$$

$$= \delta(k-l) \tag{2.13}$$

where $\delta(k-l)$ is the delta function defined as

$$\delta(k-l) \quad = \delta(n)\begin{cases} 1,\ if\ n = 0 \\ 0, otherwise \end{cases} \tag{2.14}$$

equation (2.12) shows that $\{\psi_k(t)\}_{k=0}^{N-1}$ is a set of orthogonal functions. Using this property, the OFDM signal can be demodulated.

$$= \int_0^{T_s} x(t)\, e^{-j2\pi f_k}$$

$$= \frac{1}{T_s}\int_0^{T_s} \left(\sum_{l=0}^{N-1} x_l\ \psi_l(t)\right) \bar{\psi}_k^* dt$$

$$= \sum_{l=0}^{N-1} x_l\, \delta[l-k]$$

$$= X_k \qquad (2.15)$$

this shows that for OFDM IFFT and FFT can be applied for modulation as well as demodulation. [2]

2.2 Key Advantages of OFDM Transmission

- OFDM is an efficient way to deal with multipath; for a given delay spread, the implementation complexity is significantly lower than that of a single-carrier system with an equalizer.
- In relatively slow time-varying channels, it is possible to enhance capacity significantly by adapting the data rate per Subcarrier (SC) according to the Signal to Noise Ratio (SNR) of that particular SC.
- OFDM is robust against narrowband interference because such interference affects only a small percentage of the SCs.
- OFDM makes single-frequency networks possible, which is especially attractive for broadcasting applications.

2.3 Drawbacks of OFDM Transmission

2.3.1 Orthogonality

As seen above the fact to have several carriers is actually advantageous whenever they are mathematically orthogonal. So carriers orthogonality is a constraint that can

lead to a wrong operation of OFDM systems if not respected. The orthogonality is provided by IFFT that a numerical manipulation, an error of computation could change lightly spacing between two consecutive carriers and break the orthogonality of the whole system. In this case OFDM loses all its efficiency, because the notion of orthogonality is an absolute one.

2.3.2 Synchronization

One of the crucial problems in the receiver is to sample the incoming signal correctly. If the wrong sequence of samples is processed, the Fast Fourier Transform shall not correctly recover the received data on the carriers. The problem is more embarrassing when the receiver is switched on. There is therefore a need for acquiring timing lock. If the signal transmitted is really time domain periodic, as required for the FFT to be correctly applied, then the effect of the time displacement is to modify the phase of all carriers by a known amount. This is due to the time shift theorem in Convolution transform theory.

However, the signal is not really repetitive, we have cheated and performed the mathematical transform as if it were repetitive, but then chosen different symbols and transmitted them one after the other. The effect of the time shift would then be not only to add the phase shift referred to above, but also to add some intersymbol interference with adjacent symbols. This interference could hardly degrade reception.

To avoid these problems, we decide to transmit more than one complete sequence of time samples in order to increase the tolerance in timing. It’s an additional data guard interval. It is built by repeating a set as long as channel memory of last samples taken in the original sequence. The longer the guard interval, the more rugged the system, but guard interval does not carry any useful information and its transmission leads to a penalty of power. One technique used to obtain good synchronization is to add a null (zero samples) symbol between each OFDM symbol.

2.3.3 Phase noise

At the receiver, a local oscillator can add phase noise to an OFDM signal. The phase noise could have two effects, these are: Common Phase Error (CPE) due to a rotation of the signal constellation and, Inter Carrier Interference (ICI), similar to additive

Gaussian noise. The BBC R&D have made analysis of the effects of phase noise on an OFDM signal, this analysis shows that CPE arises simultaneously on all carriers. Indeed, the signal constellation within a given symbol is subject to the same rotation for all carriers and this effect can be corrected by using reference information within the same symbol. Unfortunately, ICI is more difficult to overcome, due to the additive noise, which is different for all carriers. This difference can be interpreted as a loss of orthogonality.

2.3.4 Frequency error

An OFDM system can be subject to two types of frequency error. They are Frequency offset (as might be caused by the tolerance of the local oscillator frequency) and, Error in the receiver master clock frequency (which will cause the spacing of the demodulating carriers to be different from those transmitted). Before to find solutions to those problems, the system designer needs to determine how much residual frequency error is permissible, and understand exactly how errors affect the received signal.

Both of these error situations have been analyzed so, a frequency offset affects most carriers equally, with the very edge carrier less affected. ICI resulting from a fixed absolute frequency offset increases with the number of carriers, if the system bandwidth is kept constant. About error in the receiver clock frequency, in absence of frequency offset, it affects carriers unequally (the centre carrier suffers a little while the worst affected carrier lies close to, but not at the edge)

2.3.5 PAPR in OFDM

OFDM signals have been successfully deployed in communication systems operating in frequency selective fading channels. The attraction of OFDM is the simple equalizer structure that inverts channel distortion effects. The major drawback of conventional OFDM signals is a large PAPR. The large PAPR is due to the fact that the quadrature time domain series formed as a weighted sum of sinusoids by IFFT. By the central limit theorem, a Gaussian distribution which in turn has a complex envelope exhibiting a Rayleigh distribution with long thin tails [12].

If we consider N modulated data symbols from a particular signalling constellation, $X_k = (X_k, X_k, \dots, X_{N-1})$, over a time interval $[0, T]$, the OFDM symbol can be written as

$$x(t) = \sum_{k=0}^{N-1} X_k e^{j2\pi k f_0 t} \tag{2.16}$$

where $f_0 = \frac{1}{T}$

replacing $t = n T_b$, where, $T_b = \frac{T}{N}$, we arrive at the discrete tim e version given by

$$x_n = \sum_{k=0}^{N-1} X_k e^{j2\pi kn/N} \tag{2.17}$$

by Parseval's Theorem

$$Average\ power = E\{|x[n]|^2\} = \frac{1}{N} E\{|X[k]|^2\} \tag{2.18}$$

if all the frequency components align in phase for one particular value of n, we get

$$Max\ power = max|x[n]|^2 \leq max|X[k]|^2 \tag{2.19}$$

the PAPR of the signal, $x(t)$, is then given as the ratio of the peak instantaneous power to the average power, written as

$$PAPR = N \frac{max|X(k)|^2}{E\{|X(k)|^2\}} \tag{2.20}$$

here $E[.]$ is the expectation operator.

Say we have the same value of $X(k)$ for all k then

$$max|X(k)|^2 = E\{|X(k)|^2\} \tag{2.21}$$

$$PAPR = N \tag{2.22}$$

Equation (2.22), shows that if N is large enough, based on the central limit theorem, the real and imaginary parts of $x(t)$ have Gaussian distribution and its

envelope will follow a Rayleigh distribution. This implies a large PAPR. Equivalently, we can think of this as N sinusoids adding constructively to give a PAPR as large as N. PAPR increases as the number of subcarriers increases. [2]

2.3.6 Effects of PAPR on OFDM Signals

OFDM has large PAPR, which may saturate the power amplifier at the transmitter that means the maximum output power of the amplifier will limit the peak amplitude of the signal and this effect will produce interference both within the OFDM band and in adjacent frequency bands. With high PAPR, the conversion of OFDM signals from A/D and D/A will be more challenging. Where in band interference will increase Inter Symbol Interference (ISI) while out band interference will result in high Adjacent Channel Interference (ACI). These are undesirable phenomena in communication system. We can say that, PAPR is ruining the advantage of OFDM signal, which is said to have less ISI and immune to ICI. The threat of high PAPR is that, it may disturb the orthogonality of the OFDM signal as well. [13]

So the reduction of high PAPR is mandatory for the OFDM signal. The conventional solutions to this problem are to use a linear amplifier or to back-off the operating point of a nonlinear amplifier, both approaches resulting in a significant power efficiency penalty. Such a high PAPR necessitates the Power Amplifier (PA) be linear within wide dynamic range. The power efficiency of the PA depends on its linear dynamic range and the efficiency decreases as the dynamic range increases. Therefore it is vital for the communication system based on the OFDM to reduce the PAPR.

2.4 PAPR Reduction Using Selective Mapping Technique (SLM)

In the SLM technique, the transmitter generates a set of sufficiently different candidate data blocks, all representing the same information as the original data block, and selects the most favourable for transmission [14]. A block diagram of the SLM technique is shown in fig. 2.2. In SLM technique, each data block is multiplied by U different phase sequence, each of length N. $B_u = \lfloor B_{u,o}\, B_{u,1} \ldots B_{u,N-1} \rfloor, 1 \leq u \leq U$, resulting alternative input block sequence $X_u, 1 \leq u \leq U,$ where the multiplication

between input block sequence X and U phase sequence is component-wise vector multiplication that is

$$X_u = \lfloor X_{u,0}\, X_{u,1}, \dots, X_{u,N-1} \rfloor \quad (2.23)$$

$$= X \square B_u \quad (2.24)$$

$$= \lfloor X_0\, B_{u,0}\, , X_1\, B_{u,1}, \dots, X_{N-1}\, B_{u,N-1} \rfloor, 1 \le u \le U \quad (2.25)$$

where $\otimes$ denotes the component-wise multiplication of two vectors. The phase sequence B_u is generated by using the unit-magnitude complex number, that is

$$B_{u,n} = \mathcal{E}^{j\square_{u,n}}$$

where $\square_{u,n} \square [0,2\pi]$.

In general, binary or quaternary elements are used for $B_{u,n}$ that is $\{\pm 1\}$ or $\{\pm 1, , \pm j, \}$ where $j = \sqrt{-1}$.

IFFT should be performed for each of U input data block sequence $\{X_1, X_2, \dots, X_U\}$ to enerate U alternative OFDM signal sequences as

$$x_u = IFFT(X_u) = IIFT(X \square B_u), 1 \le u \le U \quad (2.26)$$

which bear the same input block sequence. Then, the OFDM signal sequence x_u with the minimum PAPR among U alternative OFDM signal sequences $x_u, 1 \le u \le U$, is selected and transmitted.

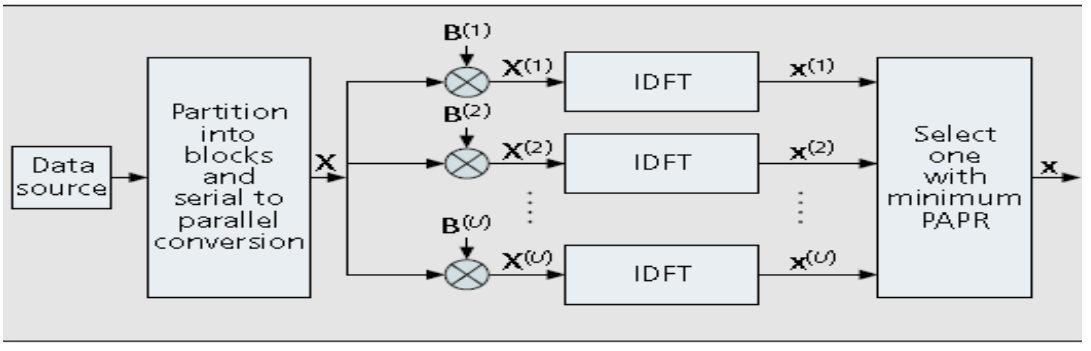

Figure 2.2 Block diagram of selective mapping technique [12]

And the information about the selected phase sequence should be transmitted to the receiver as side information. At the receiver reverse operation is performed to recover, the original data block. For implementation, the SLM technique needs $U\ IDFT$ operations, and the number of required side information bits is $log_2 U$ for each data block. This approach is applicable with all types of modulation and any number of subcarriers. The amount of PAPR reduction for SLM depends on the number of phase sequences U and the design of the phase sequences. Clearly, as U increases, the amount of PAPR reduction for the OFDM signal sequence becomes larger. But, for large U, the computational complexity becomes too high mainly due to $U\ IFFTs$. [12]

Chapter 3

IEEE 802.11a Physical Layer Model Overview

The IEEE 802.11a standard uses the 5-GHz range, which is not as interference-prone (compared to the 2.4-GHz band), due to the relatively minimal technologies operating in this domain [10]. According to the IEEE, the role of the IEEE 802.11a standard, which was approved in September 1999, is to "develop a higher speed PHY for use in fixed, moving or portable wireless local area networks". Several PHY layer technologies were investigated, and the IEEE finally decided on orthogonal frequency division multiplexing (OFDM) as the technology for transmission. This is a new encoding scheme that offers benefits over spread spectrum. In OFDM, each user transmits using 20-MHz, which is in turn divided into 52 subcarriers of 300 KHz each. The subcarriers are transmitted in parallel, with each subcarrier transmitting at a much lower rate than the total combined data rate. The receiving device processes and combines these individual signals, each one representing a fraction of the total data, to make up the actual signal.

3.1 Simulation model

In this section the block diagram of the simulation model used and the function of each block are explained.

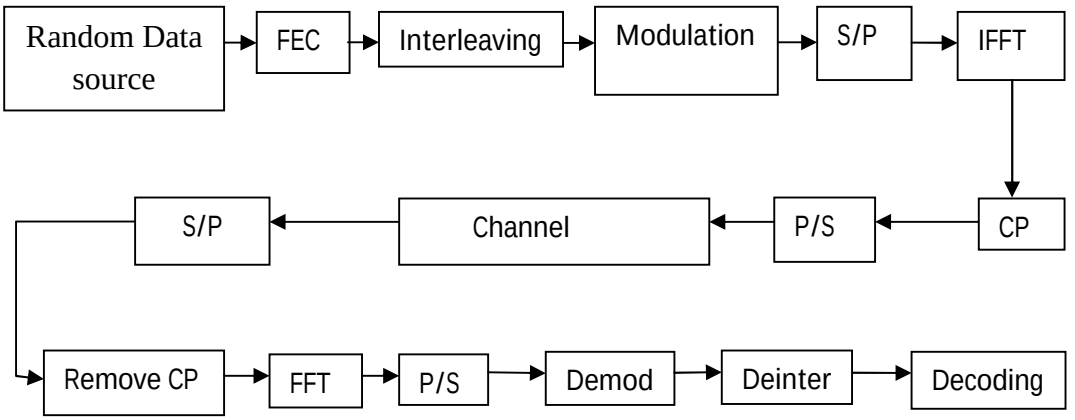

Figure 3.1: Physical layer of 802.11a

3.1.1 Source Generator

Source generation block is used to generate the information bits. The information bits are generated using MATLAB function “randint”.

3.1.2 FEC

Coding has the usefulness that it allows us to increase the rate at which information may be transmitted over a channel while maintaining a fixed error rate. Alternatively, coding allows us to reduce the information bit error rate while maintaining a fixed transmission rate. More generally, coding allows us, in principle (up to the Shannon limit) to design a communication system in which both information bit rate and error rate are independently and arbitrarily specified but subject to a constraint on bandwidth. The price we pay, for seeking to reach closer to Shannon limit, is increased hardware complexity both at the transmitter where encoding is done and at the receiver where decoding is affected. In principle, with ingenious enough coding and unlimited complexity we would be able to reach the Shannon limit. That is, we would be able to transmit at channel capacity and with an error rate which may be made as small as desired. One measure of the efficiency of a code is precisely the extent to which it allows us to approach the Shannon limit **[**15].

3.1.2.1 Convolution Coding (CC)

In block coding, the encoder accepts a $k - bit$ message block and generates an n bit code word. Thus, code words are produced on block by block basis. Clearly, provision must be made in the encoder to buffer an entire message block before generating the associated code word. There are applications, however, where the message bits come in serially rather than in large blocks, in which case the use of buffer may be undesirable. In such case the use of Convolution coding may be preferred method. [16]

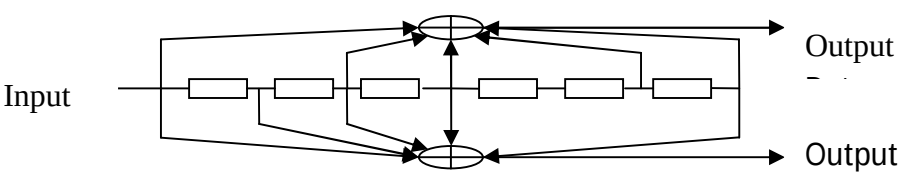

Figure 3.2: Convolutional encoder for IEE 802.11a [5].

A Convolution code introduces redundant bits into the data stream through the use of linear shift register. The information bits are input into shift register and the output encoded bits are obtained by modulo-2 addition of the input information bits and the contents of the shift register. IEEE 802.11a physical layer uses Convolution code as the mandatory FEC. The Convolutional encoder shall use the industry standard generator polynomials, g_0 = 1338 and g_1 = 1718, of rate $R = 1/2$, as shown in fig. 3.2. The bit denoted as "A" shall be output from the encoder before the bit denoted as "B." Higher rates like 2/3 and 3/4, are derived from it by employing "puncturing." Puncturing is a procedure for omitting some of the encoded bits in the transmitter (thus reducing the number of transmitted bits and increasing the coding rate) and inserting a dummy "zero" metric into the Convolutional decoder on the receive side in place of the omitted bits. For decoding the Viterbi algorithm is used.

To describe a Convolution code, one needs to characterize the encoding function $G(m)$, so that given an input sequence m, one can readily compute the output sequence U. Several methods are used for representing a Convolutional encoder. They are

- Generator/connection Representation
- Tree Diagram Representation
- State Diagram Representation
- Trellis Diagram Representation

3.1.2.2 Connection Representation

We shall use the Convolutional encoder, shown in fig. 3.3, as a model for discussing Convolutional encoders. The fig. 3.3 illustrates a $(2,1)$ Convolutional encoder with constraints length $k = 3$.

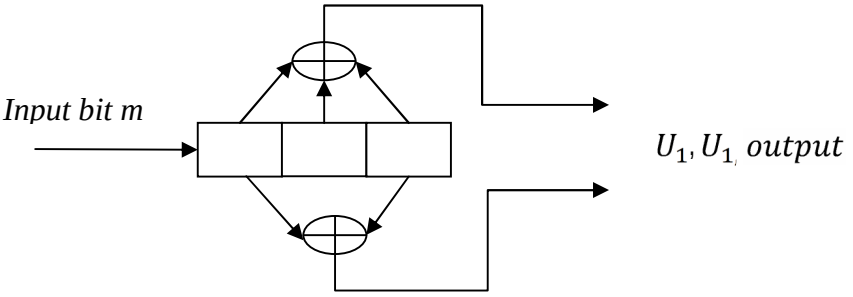

Figure 3.3: Convolutional encoder

There are two modulo-2 adders (i.e. $n = 2$); thus the code rate k/n is $1/2$. At each time, when a bit is shifted into the left most stage and bits in the register are shifted one position to the right. Next, output switch samples the output of each modulo-2 adder (i.e., first the upper adder, then the lower adder), thus forming the code symbol pair making up the branch word associated with the bit just inputted.

The sampling is repeated for each inputted bit. The choice of connections between the adders and the stages of the register gives rise to the characteristics of the code. Any change of the choice of connections result in a different code. The connections are of course, not chosen or changed arbitrarily. The problem of choosing connections to yield good distance properties is complicated and has not been solved in general.

Unlike a block code that has a fixed word length n, a Convolution code has no particular size. However, Convolution codes are often forced into a block structure by periodic truncation. This requires a number of zero bits to be appended to the end of input data sequence, for the purpose of clearing of flushing the encoding shift register of the data bits. Since the added zeros carry no information, the effective code rate falls below k/n. To keep the code rate close to k/n, the truncation period is generally made as long as practical.

3.1.2.3 Polynomial Representation

Sometimes, the encoder connections are characterized by generator polynomials. We can represent a Convolutional encoder with a set of n generator polynomials, one each of the n modulo-2 adders. Each polynomial is of degree $(k - 1)$ or less and describes the connection of the encoding shift register to that modulo-2 adder, much the same way that a connection vector does. The coefficient of each term in the $k - 1$ degree polynomial is either 0 or 1 depending on whether a connection exists or does not exist between shift register and modulo-2 adder. Generator polynomials for encoder shown in fig. 3.3 are

$$g_1 = 1\,1\,1$$

$$g_1 = 1\,0\,1$$

$$g_1(X) = 1 + X + X^2 \qquad (3.1)$$

$$g_2(X) = 1 + X^2 \quad (3.2)$$

the output sequence is found as follows

$U(X) = m(X)\, g_1(X)$ interlaced with $m(X)\, g_2(X)$.

3.1.2.4 State Representation and State Diagram

A Convolutional encoder belongs to a class of devices known as finite state machine that means machine that have a memory of past signals. The adjective finite refers to the fact that there are only a finite number of unique states that the machine can encounter. What is meant by the state of a finite state machine? In the most general sense, the state consists of the smallest amount of information that, together with a current input to the machine, can predict the output of the machine. The state provides some knowledge of the past signalling events and the restricted set of possible output in the future. A future state is restricted by past state. For a state $1/n$ Convolutional encoder, the state is represented by the contents of the rightmost $k-1$ stages. Knowledge of the state together with knowledge of the next input is necessary and sufficient to determine the next output. Let the state of the encoder at time t_i be defined as $X_i = m_{i-1}, m_{i-2}, \ldots, m_i$. The i^{th} codeword branch U_i is completely determined by state X_i and the present input bit m_i; thus the state X_i represents the past history of the encoder in determining the encoder output. The encoder state is said to be Markov, in the sense that the probabilities $P(X_{i+1}|X_i, X_{i-1})$ of being in state X_{i+1}, given all previous states, depends only on the most recent state X_i; that is the, the probability is equal to $P(X_{i+1}|X_i)$.

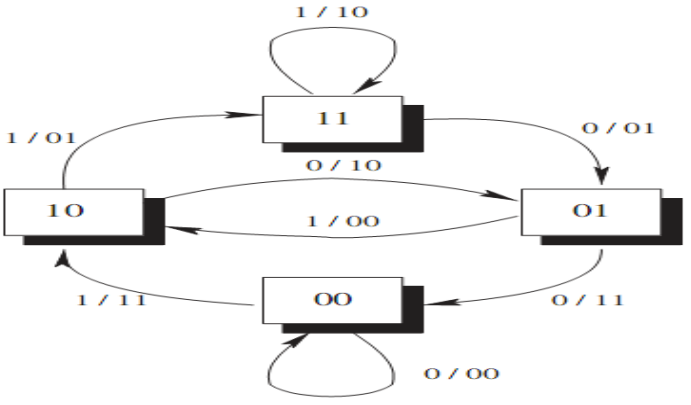

Fig 3.4: State diagram [18]

One way to represent simple encoder is with a state diagram; such a representation for the encoder in fig. 3.3 is shown in fig. 3.4. The states, shown in the boxes of the diagram, represent the possible contents of the right most $(k-1)$ stages of the register and the path between the states represent the output branch words resulting from such state transition. The state of the register are designated a= 00, b=10, c=01, d=11; the diagram shown in fig. 3.4 illustrates all the state transitions that are possible for the encoder in fig. 3.3. There are only two transitions emanating from each state, corresponding to the two possible input bits. Next to each path between states is written the output branch word associated with the state transition. In drawing the path, we use the convention that a solid line denotes a path associated with the input bit, zero and a dashed line denotes a path associated with an input bit one. Notice that it is not possible in single transition to move from a given state to any arbitrary state. As a consequence of shifting in one bit at a time, there are only two possible state transitions that the registers can make at each bit time. For example, the present encoder state is 00; the only possibilities for the state at the next shift are 00.

3.1.2.5 Tree Diagram

Although the state diagram completely characterizes the encoder, one cannot easily use it for tracking the encoder transitions as a function of time since the diagram cannot represent time history. The tree diagram adds the dimension of time to the state of diagram. The tree diagram for the Convolutional encoder shown in fig. 3.3 is illustrated in fig. 3.5

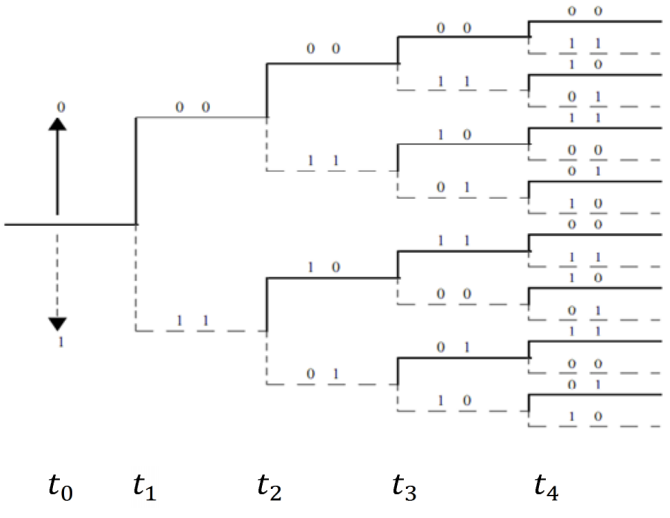

Figure 3.5: Tree diagram [18]

At each successive input bit time the encoding procedure can be described by traversing the diagram from left to right, each tree branch describing an output branch word. The branching rule for finding a codeword sequence is as follows. If the input bit is zero, its associated branch word is found by moving to the next right most branch in the upward direction. If input bit is one, its branch word is found by moving to the next rightmost branch in the downward direction. Assuming that, at initial stage contents of the encoder are zero, the diagram shows that if input bit is zero, the output branch is 00 and if the first input bit is one, the output branch is 11. Similarly, if the first input bit is one and the second input bit is a zero, the second output branch word is 10 or the first input bit is a one and second input bit is zero, second output branch is 01. Following procedure we see that the input sequence 11011 traces the heavy line drawn on the tree diagram in fig. 3.5. This path corresponds to the output code word sequence 1101010001.

3.1.2.6 Trellis Diagram

Observation of the fig. 3.5 tree diagram shows that for this example, the structure repeats itself at time t_4, after third branching (in general the tree structure repeats after k branching where k is the constraint length). We label each node in the tree of fig. 3.5 correspond to the four possible states in the shift register, as follows: a=00, b=10, c=01, and d=11.The first branching of the tree structure, at time t_1, produces a pair nodes labelled a and b. At each successive branching the number of nodes doubles. The second branching, at time t_2, results in four nodes labelled a, b, c, and d. After third branching, there are total of eight nodes: two are labelled a, two are labelled b, two are labelled c, and two are labelled d.

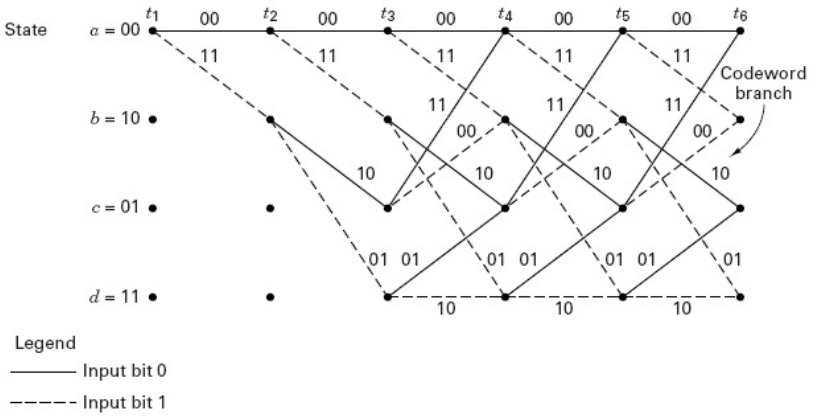

Figure 3.6: Trellis diagram [18]

We can see that all branches emanating from two nodes of the same state generate identical branch word sequences. From this point on, the upper and lower halves of the tree are identical. The reason for this should be obvious from examination of encoder in fig. 3.3. As the fourth input bit enters the encoder on left, the first input bit is ejected on the right and no longer influences the output branch words. Consequently, the input sequences 1 0 0 x y…. and 0 0 0 x y…, where the left most bit is the earliest bit, generates the same branch words after third branching. This means that any two nodes having the same state label at the same time can be merged, since all succeeding path will be indistinguishable. If we do this to tree structure of fig. 3.3, we obtain another diagram, called the trellis diagram. The trellis diagram, by exploiting the repetitive structure, provides a more manageable encoder description than does the tree diagram. The trellis diagram for the Convolutional encoder of fig. 3.3 is shown in fig. 3.6.

To draw the trellis diagram, we consider solid line as output generated by an input bit zero, and a dashed line as output generated by an input bit one. The nodes of the trellis characterize the encoder states; the first row nodes correspond to the state a= 00, the second and subsequent rows correspond to the states b= 10, c= 01 and d= 11. At each unit of time, the trellis requires 2^{k-1} nodes to represent the 2^{k-1} possible encoder states. The trellis in our example assumes a fixed periodic structure after trellis depth 3 is reached (at time t_4). In general case, the fixed structure prevails after depth k is reached. At this point and thereafter, each of the state can be entered from either of two preceding states. Also each of the states can transition to one of the two states. Of the two outgoing branches, one corresponds to an input bit zero and the other corresponds to an input bit one. On fig. 3.6, the output branch words corresponding to the state transitions appear as labels on the trellis branches. [16]

3.1.2.7 Viterbi Convolutional Decoding Algorithm

Viterbi decoder can be represented in three parts

- Find out the Hamming distance of each path.
- Add the distance of each path.
- Compare and select the shortest path.

The Viterbi decoding algorithm was discovered and analyzed by Viterbi in 1967. The Viterbi algorithm essentially performs maximum likelihood decoding; however, it reduces the computational load by taking advantage of the special structure in the code trellis.

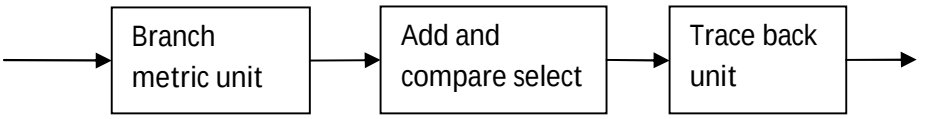

Figure 3.7: Viterbi decoder

The advantage of Viterbi decoding, compared with brute force decoding, is that the complexity of a Viterbi decoder is not a function of the number of symbols in the codeword sequence. The algorithm involves calculating a measure of similarity or distance, between the received signal, at time t_i, and all the trellis paths entering each state at time t_i. The Viterbi algorithm removes from consideration those trellis paths that could not possibly be candidates for the maximum likelihood choice. When two paths enter the same state, the one having the best metric is chosen; this path is called the surviving path. This selection of surviving path is performed for all the states. The decoder continues in this way to advance deeper into the trellis, making decision by eliminating the least likely path. The Viterbi algorithm is, in fact, maximum likelihood. Note that the goal of selecting the optimum path can be expressed, equivalently, as choosing the codeword with the maximum likelihood metric or as choosing the codeword with the minimum distance metric. [16]

3.1.2.8 Reed Solomon Codes (RS codes)

The Reed-Solomon codes are the subclass of non binary BCH (Bose Chaudhuri Hocquenghem) codes; they are usually abbreviated as RS codes. The encoder for RS code operates on multiple bits rather than individual bits unlike binary encoder which operates on single bit. Specifically, an RS (n, k) code is used to encode m-bit symbols by adding $(n - k)$ redundant symbols. When m an integer power of two, the m-bit symbols are called bytes. A popular value of m is 8; because, 8-bit RS codes are extremely powerful [17]. Reed-Solomon codes can be used as both error-correcting and erasure codes. In the error-correcting setting, we wish to transmit a sequence of

numbers over a noisy communication channel. The channel noise might cause the data sent to arrive corrupted. In the erasure setting, the channel might fail to send our message. For both cases, we handle the problem of noise by sending additional information beyond the original message. The data sent is an encoding of the original message. If the noise is small enough, the additional information will allow the original message to be recovered, through a decoding process.

Table 3.1: Parameters of a t-error-correcting RS code

Block length	$n = 2^m - 1\ symbols$
Message size	$k\ symbols$
Parity-check size	$n - k = 2t\ symbols$
Minimum distance	$d_{min} = 2t + 1\ symbols$

3.1.2.9 Arithmetic in $GF(2^r)$

In practice, we want our Reed-Solomon codes to be very efficient. In this regard, working in $GF(p)$ for some prime is inconvenient, for several reasons. Let us suppose it is most convenient if we work in blocks of 8 bits. If we work in $GF(251)$, we are not using all the possibilities for our eight bits. Besides being wasteful, this is problematic if our data (which may come from text, compressed data, etc.) contains a block of eight bits which corresponds to the number 252!. It is therefore more natural to work in a field with 2^r elements, or $GF(2^r)$. Arithmetic is this field is done by finding an irreducible (prime) polynomial $\pi(x)$ of degree r, and doing all arithmetic in $Z_2[\pi(x)]$. That is, all coefficients are modulo 2, arithmetic is done modulo $\pi(x)$, and $\pi(x)$ should not be able to be factored over $GF(2)$.

For example, for $GF(2^8)$, an irreducible polynomial is $\pi(x) = x^8 + x^6 + x^5 + x + 1$. A byte can naturally be thought of as a polynomial in the field. For example, by letting the least significant bit represent x^0 and the most significant bit represent x^i, we have that the byte 10010010 represents the polynomial $x^7 + x^4 + x$. Adding in $GF(2^r)$ is easy: since all coefficients are modulo 2, we can just XOR two bytes together. For example

$$10010010 + 10101010 = 00111000$$

$$(x^7 + x^4 + x) + (x^7 + x^5 + x^3 + x) = (x^5 + x^4 + x^3) \quad (3.3)$$

moreover, subtracting is just the same as adding. Multiplication is slightly harder, since we work modulo $\pi(x)$. As an example

$$(x^4 + x)(x^8 + x^2) = x^8 + x^6 + x^5 + x + 1 \quad (3.4)$$

however, we must reduce this so that we can fit it into a byte. As we work modulo $\pi(x)$, we have that $\pi(x) = 0$, or $x^8 = x^6 + x^5 + x + 1$. Hence

$$(x^4 + x).(x^4 + x^2) = x^8 + x^6 + x^5 + x^3 \quad (3.5)$$

$$= (x^6 + x^5 + x + 1) + x^6 + x^5 + x^3 \quad (3.6)$$

$$= x^3 + x + 1 \quad (3.7)$$

and hence

$$00010010 \times 00010100 = 00001011.$$

Rather than compute these products on the fly, all possible 256×256 pairs can pre-computed once in the beginning, and then all multiplications are done by just doing a lookup in the multiplication lookup table. Hence by using memory and pre-processing, one can work in $GF(2^8)$ and still obtain great speed. Reed-Solomon codes work exactly the same over $GF(2^r)$ as they do over $GF(P)$. [17]

3.1.3 Interleaver

Interleaving can be employed in digital data transmission technologies to mitigate the effect of burst errors. When too many errors exist in one code word, due to a burst error, the decoding of a code word cannot be done correctly. To reduce the effect of burst error, the bits in one code word are interleaved before being transmitted. When interleaving occurs the place of bits will change, which means that a burst error can not disturb a huge part of one code word [15]. Fig. 3.8 illustrates the effect of interleaving at the transmitter. This example explains that only a small part of each code word is distorted with interleaving, so the decoding of code word can be done correctly. All encoded data bits shall be interleaved by a block interleaver with a block size corresponding to the number of bits in a single OFDM symbol N_{CBPS}.

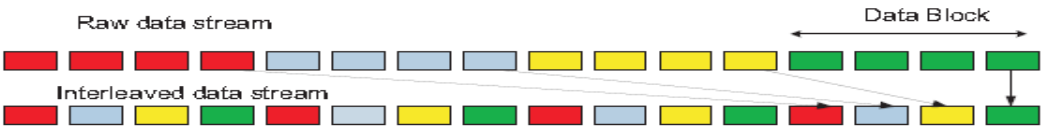

Figure 3.8: Transmission with interleaving

The interleaver is defined by a two-step permutation. The first permutation ensures that adjacent coded bits are mapped onto nonadjacent subcarriers. The second ensures that adjacent coded bits are mapped alternately onto less and more significant bits of the constellation and, thereby, long runs of low reliability bits are avoided. We shall denote by *k* the index of the coded bit before the first permutation; *i* shall be the index after the first and before the second permutation, and *j* shall be the index after the second permutation, just prior to modulation mapping.

The first permutation is defined by the rule

$$i = (N_{CBPS}/16)(k \bmod 16 + floor\left(\frac{k}{16}\right)\ k = 0,1,\dots,N_{CBPS} - 1 \qquad (3.8)$$

the function floor (.) denotes the largest integer not exceeding the parameter. The second permutation is defined by the rule

$$j = s \cdot floor\left(\frac{i}{s}\right) + \left(i + N_{CBPS} - floor\left(16 \cdot \frac{i}{N_{CBPS}}\right)\right) mods\ i = 0,1,\dots,(N_{CBPS} - 1) \qquad (3.9)$$

the value of s is determined by the number of coded bits per subcarrier, NBPSC

$$s = max\ (N\_CBPS/2,1) \qquad (3.10)$$

the deinterleaver, which performs the inverse relation, is also defined by two permutations. Here we shall denote by *j* the index of the original received bit before the first permutation; *i* shall be the index after the first and before the second permutation, and *k* shall be the index after the second permutation, just prior to delivering the coded bits to the Convolutional decoder. The first permutation is defined by the rule

$$i = s \times floor\left(\frac{j}{s}\right) + \left(j + floor\left(16 \times \frac{j}{N_{CBPS}}\right)\right) mods \quad j = 0,1, \ldots, (N_{CBPS} - 1) \tag{3.11}$$

where s is defined in Equation (3.9). This permutation is the inverse of the permutation described in Equation (3.8). The second permutation is defined by the rule

$$k = 16 \times i - (N_{CBPS} - 1) floor\left(16 * \frac{i}{N_{CBPS}}\right) \quad i = 0,1, \ldots N_{CBPS} - 1 \tag{3.12}$$

this permutation is the inverse of the permutation described in Equation (3.8). [5]

3.1.4 Subcarrier Modulation

The coded bit stream is modulated into symbols to increase the efficiency of the communication system. Modulation of the signal changes the amplitude, phase and frequency of that signal. With OFDM, only the phase and amplitude is varied. The frequency is left constant to ensure the orthogonal aspect of the sub-carriers. The situation and application controls the type of modulation scheme chosen. Through the conversion of bits to symbols, a complex number represents one or more bit, depending on the scheme chosen. The modulation schemes used in OFDM communication schemes are BPSK, QPSK, 16-QAM and 64-QAM. Each scheme maps a certain number of bits to a symbol. This can be seen in their constellation maps. For BPSK, one bit represents a symbol whilst QPSK has two bits corresponding to the same symbol. 16-QAM has four bits equating to a symbol and 64-QAM has six bits per symbol. The Bit Error Rate (BER) increases for the same SNR level as the bit per symbol mapping criteria increases. The SNR needs to be higher so the removal of the bits in the receiver can be done effectively. This is due to the smaller phase difference that each modulation scheme has when the numbers of points in the constellation map increases. As the number of points increases, the average power of the constellation increases as well. The average power equation

$$P_{ave} = \frac{1}{M} \sum_{k=1}^{M} |C_k|^2 \tag{3.13}$$

where M is the number of points in the map and C_k is the power of all the M points in the map. From the formula above, it is very easy to see that a direct relationship exists between the number of points and the power of the signal. As the power of the signal can vary with the number of points, the probability of a bit error varies as well. The equation for the probability of an erroneous bit is

$$P_b = Q\left(\sqrt{\frac{E_b}{N_0}}\right) \tag{3.14}$$

where, Q is the Probability Density Function of a zero mean, normal, random variable, E_b is the energy of the bit and N_0 is the power of the noise. For BPSK, there are only two outcomes for a '0' and a '1'. These results are separated by 180°. The constellation map for BPSK is shown in fig.3.9. When the data goes through the noisy channel, the data points will not be exactly on the constellation point as above. The difference between the exact and where it does occur is called the vector error. With BPSK, it does not have any imaginary factors as part of the complex number.

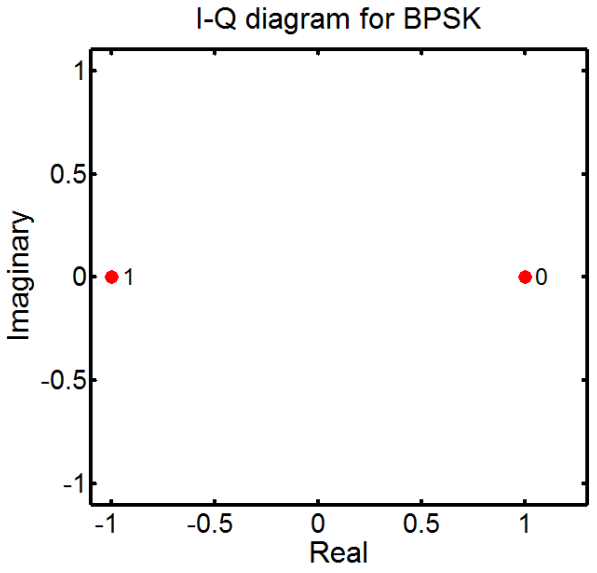

Figure 3.9: BPSK constellation map

This leaves the result to be on the real axis either side of the zero mark. The receiver can decide what the data point is supposed to be, either a '0' or a '1', depending on which side of the zero point the data is. For QPSK, there are four points in the constellation map. Each point has a real part and an imaginary part that makes

up the complex number. This means, besides having points on either side of the zero line in the real dimension, it also has points either side of the zero line in the quadrature dimension. The area where a data point is, after being affected by noise, is only a quarter of the map if it is to be analysed as correct. If the data point has a phase change greater than 90°, it will fall into a different quadrant, the receiver will interpret it as a different data point and an error will occur. To ensure errors are minimised, the SNR needs to be larger than for the BPSK scheme. The receiver must decide whether the data point is one of four points as opposed to one of two points in the BPSK modulation scheme. The constellation map for QPSK is shown in fig 3.10.

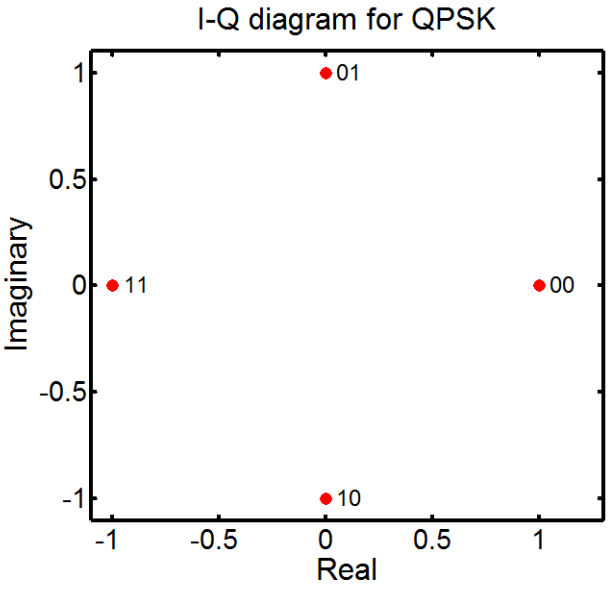

Figure 3.10: QPSK constellation map.

The 16-QAM modulation scheme has sixteen points of which the receiver needs to ensure the data is correct. This allows for only a phase change of 45° before it becomes an error. As well as signal phase changes to depict different data points, QAM schemes, also, changes the amplitude of the signal. Two aspects of the signal are needed to be correct to ensure the correct data is retrieved as opposed to one for the PSK schemes.

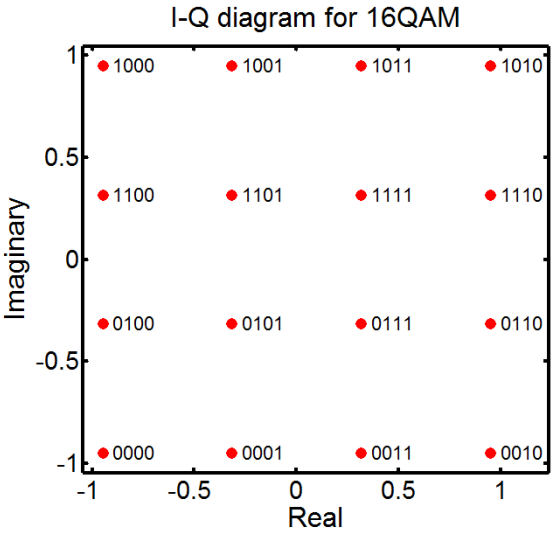

Figure 3.11: 16-QAM constellation map

The SNR of the signal needs to greater to enable the receiver to interpret the signal correctly. If the amplitude or phase varies, an error can result. The constellation map for 16-QAM is shown in fig. 3.11.

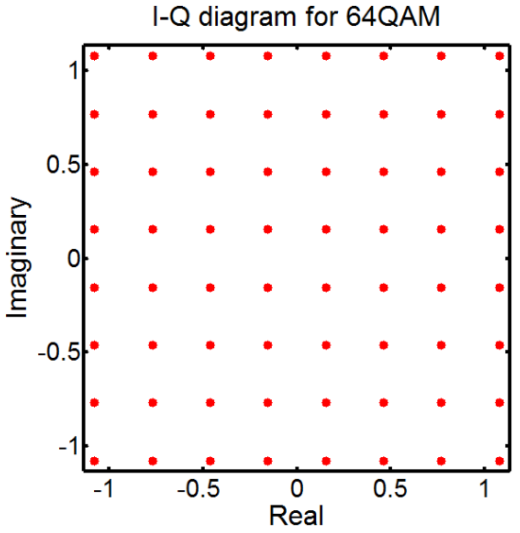

Figure 3.12: 64-QAM constellation map

The final modulation scheme used is 64-QAM. This scheme has sixty-four data points in its constellation map. The phase difference that the scheme allows before an error would occur is 22.5°. This is half of the previous scheme, 16-QAM, so the data points need to be more precise to ensure the receiver correctly deciphers

the signal. As well, there are four levels of amplitude the scheme uses. The signal will need a larger SNR to ensure the data is correctly extracted from the signal. The constellation scheme for 64-QAM is shown in fig. 3.12. [17]

3.1.5 Pilot Subcarriers

The transmitted signal, passing through a wireless channel, will be affected by a frequency and phase shift as well as noise. To help a receiver to extract the data from the received signal, pilot tones are inserted into the OFDM signal. These signals are positioned throughout the OFDM symbol for the maximum effect of being able to help the receiver detect a change in the frequency or phase of the transmitted signal. The synchronisation data the pilots carry, add to the overall data that is sent, but are considered overhead signals. The synchronisation of the receiver to the transmitted signal enables the receiver to extract the required data.

In IEEE 802.11a for each OFDM symbol, four of the subcarriers are dedicated to pilot signals in order to make the coherent detection robust against frequency offsets and phase noise. These pilot signals shall be put in subcarriers –21, –7, 7 and 21. The pilots shall be BPSK modulated by a pseudo binary sequence to prevent the generation of spectral lines. [5]

3.1.6 OFDM modulation

The stream of complex numbers is divided into groups of $N_{SD} = 48$ complex numbers. We shall denote this by writing the complex number $d_{k,n}$ which corresponds to subcarrier k of OFDM symbol n, as follows

$$d_{k,n} = d_{k+n\cdot N_{SD}}, \quad k = 0, \ldots N_{SD} - 1, n = 0, \ldots N_{SYM} - 1 \tag{3.15}$$

an OFDM symbols, $r_{DATA,n}(t)$, is defined as

$$r_{DATA,n}(t) = w_{TSYM}(t)\left[\sum_{k=0}^{N_{SD}-1} d_{k,n}\exp\left[\left(j2\pi M(k)\Delta_F(t - T_{GI})\right) + P_{n+1}\right.\right.$$

$$\left.\left. + \sum_{k=-N_{ST}/2}^{N_{ST}/2} P_k\exp(j2\pi\Delta_F(t - T_{GI}))\right]\right] \tag{3.16}$$

where the function, $M(k)$defines a mapping from the logical subcarrier number 0 to 47 into frequency offset index -26 to 26, while skipping the pilot subcarrier locations and the 0^{th}(dc) subcarrier. [5]

The contribution of the pilot subcarriers for the n^{th} OFDM symbol is produced by Fourier transform of sequence P, given by

$$P_{-26,26} = \{0, 0, 0, 0, 0, 1, 0, 0, 0, 0, 0, 0, 0, 0, 0, 0, 0, 0, 0, 1, 0, 0, 0, 0, 0, 0, 0,$$
$$0, 0, 0, 0, 0, 0, 1, 0, 0, 0, 0, 0, 0, 0, 0, 0, 0, 0, 0, 0, –, 0, 0, 0, 0, 0\}$$

the concatenation of N_{SYM} OFDM symbols can now be written as

$$r_{DATA}(t) = \sum_{n=0}^{N_{SYM}-1} r_{DATA,n}(t - nT_{SYM}) \qquad (3.17)$$

3.1.7 Cyclic Prefix

Since the spectra of an OFDM signal is not strictly band limited ($sinc(f)$ function), linear distortions such as multipath cause each sub-channel to spread energy into the adjacent channels and consequently cause Inter Symbol Interference (ISI) [2]. A simple solution is to increase the symbol duration or the number of carriers so that the distortion becomes insignificant. However, this method may be difficult to implement in terms of carrier stability, Doppler shift, FFT size and latency.

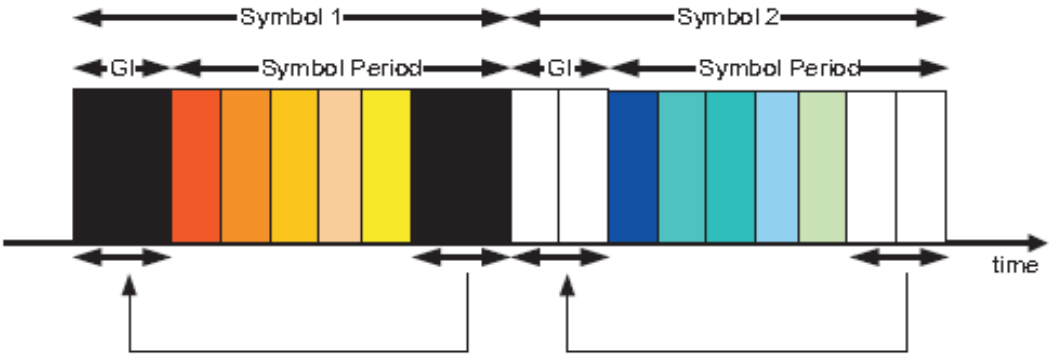

Figure 3.13: Cyclic Prefix Insertion [2]

One way to prevent ISI is to create a cyclically extended guard interval, where each OFDM symbol is preceded by a periodic extension of the signal itself. As shown in the fig 3.13, the total symbol duration is $T_{total} = T_g + T$, where T_g, is the guard

interval GI and T is the useful symbol period. When the guard interval is longer than the channel impulse response, or the multipath delay, the ISI can be eliminated. However, the ICI, or in-band fading, still exists. The ratio of the guard interval to useful symbol duration is application dependent. Since the insertion of guard interval will reduce data throughput, so T_g is usually less than $T/4$.

3.1.8 Radio Channel

For the simulations purpose different channels are used like AWGN, Rayleigh fading, Ricean fading and Nakagami fading. In chapter 4 these channels are explained in detail.

3.1.9 IFFT

Once the pilots have been inserted into the data symbols, the data is put through an Inverse Fast Fourier Transform (IFFT). This maps the complex data symbols to a Time Domain OFDM symbol. The OFDM symbol is made of a number of discrete, baseband and orthogonal sub-carriers, which carry the data symbols and other, required timing information. Not all sub-carriers are used for data and pilot information. There are some sub-carriers that are used as guard barriers and preamble at the start and finish of the OFDM symbol. To enable the most efficient use of the IFFT function, the number of sub-carriers is kept to a power of two, namely 2^n. Prior to the advent of Digital Signal Processors (DSPs), which allow the IFFT to be performed in a single chip, a bank of mixers, oscillators and filters performed this function. This amount of equipment meant that the size and weight were limiting factors in the use of this type of communication.

An inverse Fourier transform converts the frequency domain data stream into the corresponding time domain. Then a parallel to serial convertor is used to transmit time domain samples of one symbol. The Fast Fourier Transformation (FFT) is used to convert data in time domain to the frequency domain at the receiver. [18]

3.2 Simulation Parameters

Table 3.2: Simulation parameters

Parameter	**Value**
Nominal Channel Bandwidth, BW	20 MHz
N_{SD}:Number of data subcarriers	48
N_{SP}:Number of pilots subcarriers	4
N_{ST}:Number of total subcarriers	52($N_{SD} + N_{SP}$)
Δ_f:Subcarrier frequency spacing	0.3125MHz(20MHz/64)
T_{FFT}: IFFT/FFT period	3.2 µs (1/Δ_f)
T_{GI} GI duration	0.8 µs (T_{GI}/4
T_{SYM}: Symbol interval	4.0 µs(T_{GI}+T_{FFT})
NFFT: FFT size	64

CHAPTER 4

CHANNEL IMPAIRMENTS AND MODELS

4.1Channel Impairments

Wireless channel is always very unpredictable with harsh and challenging propagation situations. Wireless channel is very different from wireline channel in a lot of ways. Multipath reception is the unique characteristic of wireless channels. Together with multipath, there are other serious impairments present at the channel, namely propagation path loss, shadow fading, Doppler spread, time dispersion or delay spread, etc.

4.1.1 Multipath

Multipath is the result of reflection of wireless signals by objects in the environment between the transmitter and receiver. The objects can be anything present on the signal travelling path, i.e. buildings, trees, vehicles, hills or even human beings. Thus, multipath scenario includes random number of received signal from the same transmission source; depending on the location of transmitter and receiver, a direct transmission path referred to as the Line Of Sight (LOS) path may be present or may not be present. When LOS component is present (or when one of the components is much stronger than others), then the environment is modelled as Ricean channel, and when no LOS signal is present, the environment is described as Rayleigh channel. Multi-paths arrive at the receiver with random phase offsets, because each reflected wave follows a different path from transmitter to reach the receiver. The reflected waves interfere with direct LOS wave, which causes a severe degradation of network performance. The resultant is random signal fades as the reflections destructively (and/or constructively) superimpose one another, which effectively cancels part of signal energy for a brief period of time. The severity of fading will depend on delay spread of the reflected signal, as embodied by their relative phases and their relative power. [19]

A common approach to represent the multipath channel is channel impulse response which gives us the delay spread of the channel. Delay spread is the time spread between the arrival of the first and last multipath signal seen by receiver. In a

digital system, delay spread can lead to ISI. In fig. 4.1, delay spread amounts to τ_{max} is shown. It is noted that delay spread is always measured with respect to the first arriving component. Let's assume a system transmitting in the time intervals T_{sym}. The longest path with respect to the earliest path arrives at the receiver with a delay of τ_{max}; in other words, the last path arrives τ_{max} seconds after the first path arrives. This means that a received symbol can theoretically be influenced by previous symbols, which is termed as ISI.

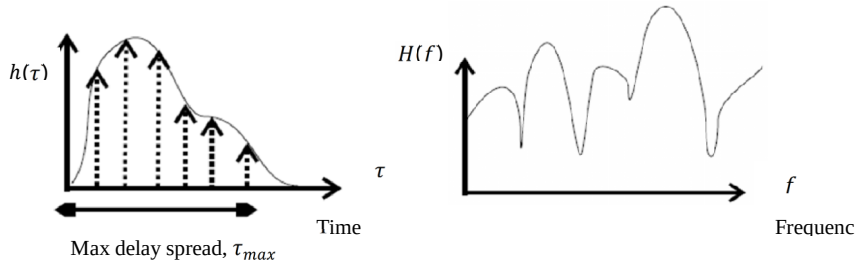

Channel response in Time Channel response in Frequency

Figure 4.1: Channel Impulse Responses and Corresponding Frequency Response [20]

With high data rate, T_{sym} can be very small; thus the number of symbols that are affected by ISI can be in multiple of tens or more. Combating the influence of such large ISI at the receiver is very challenging and sometimes may become unattainable at very severe channel conditions [20].

4.1.2 Doppler Effect

Due to Doppler Effect, if a transmitter is moving away from a receiver, the frequency of the received signal is lower than the one sent out from the transmitter; otherwise, the frequency is increased. In wireless communications, there are many factors that can cause relative movement between a transmitter and a receiver. It can be the movement of a mobile such as a cell phone; it can be the movement of some background objectives, which causes the change of path length between the transmitter and the receiver. The lengths of signal path are often different, which correspond to different movement speeds of transmitter signals, and in turn different frequency shifts on the signal paths. As a result, a frequency spread is caused in the signal spectrum. [21]

Corresponding to Doppler spectrum spread, there is a concept called coherence time, which is related to the reciprocal of the maximum Doppler shit. Coherence time is used to measure a time interval, in which a smaller amount of fading is occurred. Specifically, if the baseband signal varies faster than the coherence time, the distortion from Doppler spread fading is negligible. Such a situation is called slow fading. Otherwise, if the baseband signal varies more slowly than the coherence time, the distortion from Doppler spread fading may be significant. This situation is called fast fading.

Let us consider mobile user at position x, moving with velocity V, with signal arriving at angleθ. With a nominal carrier frequency of f_0 the received signal is

$$r(t) = Ae^{j(2\pi f_0 t - \beta x cos\theta)} \tag{4.1}$$

with phase (where $\beta = 2\pi/\lambda = wave\,number$)

$$\square(t) = 2\pi f_0 t - \beta V t cos\theta \tag{4.2}$$

and resulting Doppler frequency

$$f_D = \left(\frac{V}{C}\lambda\right) cos\theta \tag{4.3}$$

another way: from physics, for a radial (approaching) velocity V_r

$$f_D = f_0 \frac{1}{\frac{c}{V_r} - 1} = \frac{f_0 V_r}{c - V_r} \approx \frac{f_0 V_r}{c} \tag{4.4}$$

but $V_r = V cos\theta$ and $c = f_0\lambda$ so

$$f_D = \frac{V}{\lambda}\, cos\theta \tag{4.5}$$

often, V and θ will vary with time, so f_D will vary corresponding, causing Doppler spread. Often this is modelled statically. In general, the Doppler spread characterizes the rate of channel variations. [21]

4.1.2.1 Amplitude Variation Due To Motion

Now consider the case where two incoming waves arrives at the mobile at angle of 0

and θ. Assume that they are of equal amplitude. Then, from equation 4.1, the received signal is

$$r(t) = Ae^{j2\pi f_0 t\left(e^{-j\alpha}+e^{-j\alpha\, cos\theta}\right)} \tag{4.6}$$

where $\alpha = \beta x$ This can be expressed as

$$r(t) = Ae^{j2\pi f_0 t\left(e^{-j\alpha(U+D)}+e^{-j\alpha(U-D)}\right)} \tag{4.7}$$

$$U = (1 + cos\theta)/2, D = (1 - cos\theta)/2$$

factoring, we have

$$r(t) = A\ e^{j2\pi f_0 t\, e^{-j\alpha U\left(e^{-j\alpha D}+e^{-j\alpha D}\right)}} \tag{4.8}$$

notice that

$$e^{-j\alpha D} + e^{-j\alpha D} = 2\cos\left[\frac{\alpha(1 - cos\theta)}{2}\right] \tag{4.9}$$

so

$$r(t) = Ae^{j2\pi f_0 t\, e^{-j\beta x\left(\frac{1+cos\theta}{2}\right)\left(2cos\left[\frac{\beta x(1-cos\theta)}{2}\right]\right)}} \tag{4.10}$$

thus the phase of signal due to Doppler is

$$\square(t) = \frac{1}{2}\beta x(1 + cos\theta) \tag{4.11}$$

and the Doppler frequency is

$$f_D = \frac{1}{2\pi}\frac{1}{2}\frac{2\pi}{\lambda}V(1 + cos\theta) = \frac{V}{2\lambda}(1 + cos\theta) \tag{4.12}$$

but the signal amplitude fluctuates due to multipath according to

$$\theta_{sw} = \frac{\beta x}{2}(1 - cos\theta) \tag{4.13}$$

$$f_{sw} = \frac{V}{2\lambda}(1 - cos\theta) \tag{4.14}$$

4.1.3 Shadow Fading or Shadowing

Shadow fading is another troublesome effect of wireless channel. Wireless signals are obstructed by large obstacles, like huge buildings, high hills, etc. These large objects cause reflections off their surface and attenuation of signals passing through them, resulting in shadowing, or shadow fading. These shadows can result in large areas with high path loss, causing problems with communications. The amount of shadowing depends on the size of the object, the structure of the material, and the frequency of the RF (Radio Frequency) signal. Large attenuations by huge obstacles can result in deep fading behind them. Under this condition, most of the received signal energy comes from reflected and diffracted paths of the original signal, because LOS is absent due to large object between the transmitter and the receiver.

4.1.4 Delay spread

The different signal paths between a transmitter and a receiver correspond to different transmission times. For an identical signal pulse from the transmitter, multiple copies of signals are received at the receiver at different moments. The signals on shorter paths reach the receiver earlier than those on longer paths. The direct effect of these un-simultaneous arrivals of signal causes the spread of the original signal in time domain. This spread is called delay spread [22]. The delay spread puts a constraint on the maximum transmission capacity on the wireless channel. Specifically, if the period of baseband data pulse is larger than that of delay spread, inter-symbol interference (ISI) will be generated at the receiver. That is, the data signals on two neighbouring pulse periods are received at the same time, which causes the receiver not to be able to distinguish them. Corresponding to the concept of delay spread, there is a term called coherence bandwidth used to measure the up-limit bandwidth that can be transmitted for a channel to be free of ISI. Coherence bandwidth is defined as 10% of the reciprocal of root mean square (RMS) delay spread. If the bandwidth of a transmitter signal is less than the channel coherence bandwidth, the channel shows flat fading to be free of ISI. Otherwise, the channel shows frequency selective fading, and may suffer from ISI.

In communications, the delay spread is a measure of the multipath richness of a channel. In general, it can be interpreted as the difference between the time of

arrival of the first significant multipath component (typically the line of sight component) and the time of arrival of the last multipath component. It is mostly used in the characterization of wireless channels, but the same concept applies to any other multipath channel (e.g. multipath in optical fibres). The delay spread can be characterized through different metrics, although the most common one is the root mean square (RMS) delay spread. According to Goldsmith [23], let $A_c(\tau)$ be the power delay profile of a channel. Then, the mean delay of the channel is

$$\bar{\tau} = \frac{\int_0^\infty \tau A_c(\tau) d\tau}{\int_0^\infty A_c(\tau) d\tau} \tag{4.15}$$

thus, the RMS delay spread is

$$\tau_{rms} = \sqrt{\frac{\int_0^\infty (\tau - \bar{\tau})^2 A_c(\tau) d\tau}{\int_0^\infty A_c(\tau) d\tau}} \tag{4.16}$$

4.2 Channel Models

Radio technologies have undergone increasingly rapid evolutionary changes in the recent past. As technology progresses to take advantages of more complex channel characteristics, the channel modelling required to emulate the radio environment for testing becomes both more critical and more complex. For instance, when bandwidths are increased (to Support higher data rates) receivers become more susceptible to Inter Symbol Interference (ISI). To ensure that measurements in the lab accurately correlate to the Quality of the user's experience, channel models must account for all the aspects of the practical radio environment.

4.2.1 Additive white Gaussian noise (AWGN)

It is a channel model in which the only impairment to communication is a linear addition of wideband or white noise with a constant spectral density (expressed as watts per hertz of bandwidth) and a Gaussian distribution of amplitude. The model does not account for fading, frequency selectivity, interference, nonlinearity or dispersion. However, it produces simple and tractable mathematical models which are useful for gaining insight into the underlying behavior of a system before these other

phenomena are considered. Wideband Gaussian noise comes from many natural sources, such as the thermal vibrations of atoms in conductors (referred to as thermal noise or Johnson Nyquist noise), shot noise, black body radiation from the earth and other warm objects, and from celestial sources such as the Sun.

The AWGN channel is a good model for many satellite and deep space communication links. It is not a good model for most terrestrial links because of multipath, terrain blocking, interference, etc. However, for terrestrial path modeling, AWGN is commonly used to simulate background noise of the channel under study, in addition to multipath, terrain blocking, interference, ground clutter and self interference that modern radio systems encounter in terrestrial operation.

Basic characteristic of the AWGN channels are

- The noise is additive, i.e., the received signal equals the transmit signal plus some noise, where the noise is statistically independent of the signal.
- The noise is white, i.e., the power spectral density is flat, so the autocorrelation of the noise in time domain is zero for any non-zero time offset.
- The noise samples have a Gaussian distribution.

Additive white Gaussian noise (AWGN) is the commonly used to transmit signal while signals travel from the channel and simulate background noise of channel.

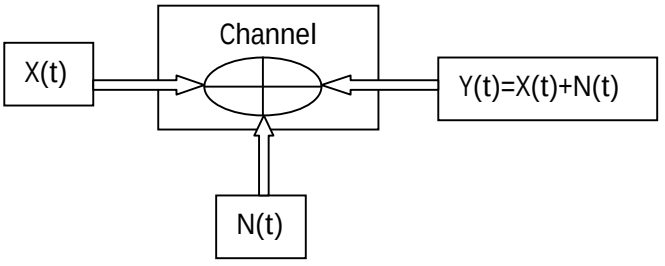

Figure 4.2: Received Signal through an AWGN channel

The mathematical expression in received signal $Y(t) = X(t) + N(t)$ is shown in fig. 4.2 that passed through the AWGN channel where s(t) is transmitted signal and n(t) is background noise [24]. Where $X(t)$ is the input waveform, regarded as a real

random process, and $N(t)$ is a real white Gaussian noise process with single-sided noise power density N_0 which is independent of $X(t)$. Moreover, the input $X(t)$ is assumed to be both power-limited and band-limited. The average input power of the input waveform $X(t)$ is limited to some constant P. The channel band B is a positive-frequency interval with bandwidth W Hz. The channel is said to be baseband if $B = [0, W]$, and passband otherwise. The (positive-frequency) support of the Fourier transform of any sample function $X(t)$ of the input process $X(t)$ is limited to B. The signal-to-noise ratio SNR of this channel model is then

$$SNR = P/N_0W \tag{4.17}$$

where N_0W is the total noise power in the band B. The parameter N_0 is defined by convention to make this relationship true; i.e., N_0 is the noise power per positive-frequency Hz. Therefore the double-sided power spectral density of $N(t)$must be $S_{nn}(f) = \frac{N_0}{2}$, at least over the bands $\pm B$.

4.2.1.1 Gaussian distribution

A Gaussian random variable is one whose probability density function can be written in the general form

$$f_x(x) = \frac{1}{\sqrt{2\pi\sigma^2}} \frac{e^{-(x-m)^2}}{2\sigma^2}, -\infty < x < \infty \tag{4.18}$$

The PDF of the Gaussian random variable has two parameters, m and σ, which have the interpretation of the mean and standard deviation respectively. The parameter σ^2 is referred to as the variance. In general, the Gaussian PDF is centred about the point $x = m$ and has a width that is proportional to σ. The CDF is required whenever we want to find the probability that a Gaussian random variable lies above or below some threshold or in some interval. The CDF of a Gaussian random variable is written as. [25]

$$F_x(x) = \int_{-\infty}^{x} \left(\frac{1}{\sqrt{2\sigma^2\pi}}\right) e^{-(y-m)^2/2\sigma^2} dy \tag{4.19}$$

it can be shown that it is impossible to express this integral in closed form. The fallowing fig. 4.3 (a) and (b) shows the PDF and CDF of a Gaussian random variable.

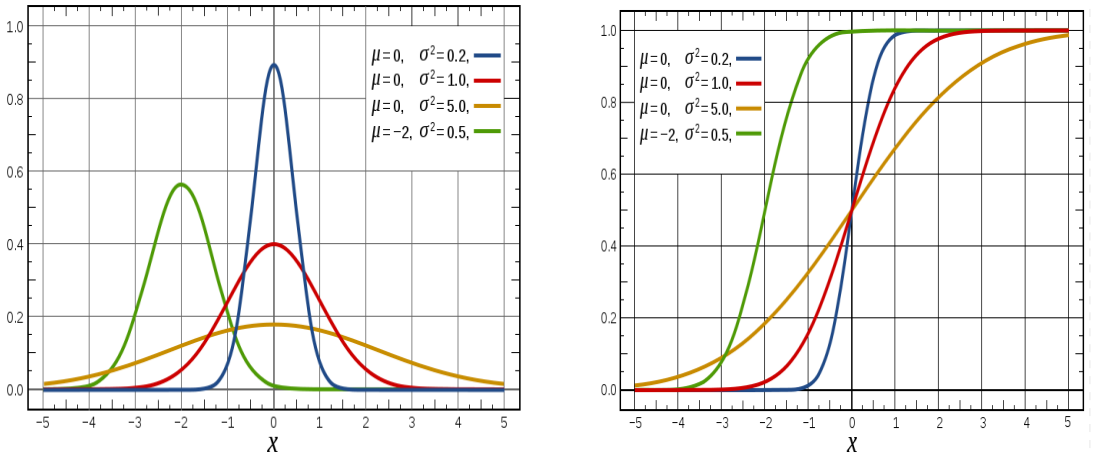

Figure 4.3: (a) PDF (b) CDF of Gaussian distribution [25]

Because Gaussian random variables are so commonly used in such a wide variety of applications, it is standard practice to introduce a shorthand notation to describe a Gaussian random variable $X \sim N(m, \sigma^2)$. This is read X is distributed normally (or Gaussian) with mean m, and variance σ^2.

4.2.2 Rayleigh fading channel

Rayleigh fading is a statistical model for the effect of a propagation environment on a radio signal, such as that used by wireless devices. Rayleigh fading models assume that the magnitude of a signal that has passed through such a transmission medium (also called a communications channel) will vary randomly, or fade, according to a Rayleigh distribution the radial component of the sum of two uncorrelated Gaussian random variables.Rayleigh fading is viewed as a reasonable model for tropospheric and ionospheric signal propagation as well as the effect of heavily built-up urban environments on radio signals. Rayleigh fading is most applicable when there is no dominant propagation along a line of sight between the transmitter and receiver. [26]

4.2.2.1 Rayleigh distribution

A Rayleigh random variable has a one sided PDF. The form of the PDF and CDF are given (for any $\sigma > 0$) by

$$f_x(x) = \left(\frac{x}{\sigma^2}\right) \exp\left(-\frac{x^2}{2\sigma^2}\right) u(x) \qquad (4.20)$$

$$F_x(x) = 1 - exp\left(-\frac{x^2}{2\sigma^2}\right) \quad (4.21)$$

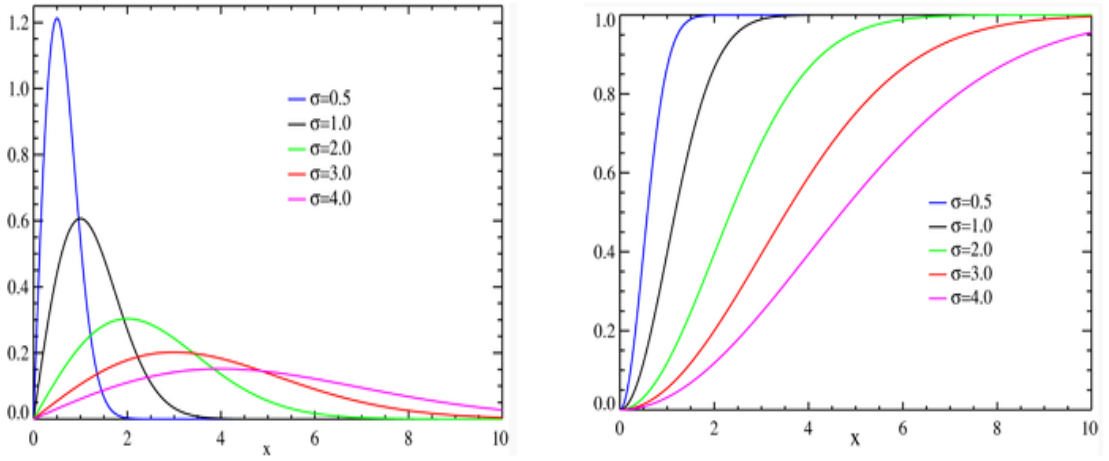

Figure 4.4: (a) PDF (b) CDF of Rayleigh random variable [27]

4.2.3 Ricean fading channel

Ricean fading channel is a stochastic model for radio propagation anomaly caused by partial cancellation of a radio signal by itself, the signal arrives at the receiver by two different paths (hence exhibiting multipath interference), and at least one of the paths is changing (lengthening or shortening).

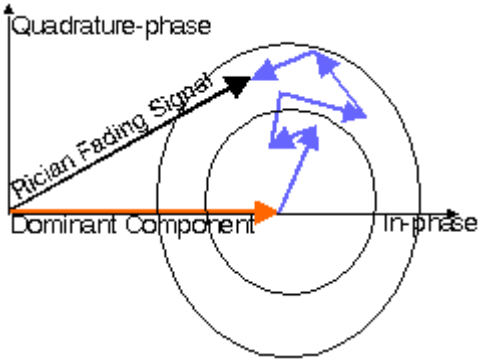

Figure 4.5: Ricean fading model [27]

Ricean fading occurs when one of the paths, typically a line of sight signal, is much stronger than the others. In Ricean fading, the amplitude gain is characterized by a Rician distribution. In Ricean fading, a strong dominant component is present. Similar to the case of Rayleigh fading, the in-phase and quadrature phase component

of the received signal are jointly Gaussian random variables. However, in Ricean fading the mean value of (at least) one component is non-zero due to a deterministic strong wave.

4.2.3.1 Ricean distribution

A Ricean random variable is closely related to the Rayleigh random variable (in fact, the Rayleigh distribution is a special case of the Ricean distribution). The functional form of the PDF for a Ricean random variable is given (for any $v > 0$ and any $\sigma > 0$) by

$$f_x(x) = \left(\frac{x}{\sigma^2}\right) \exp\left(-x^2 + \frac{v^2}{2\sigma^2}\right) I_0\left(\frac{vx}{\sigma^2}\right) u(x) \qquad (4.22)$$

in this expression, the function $I_0(x)$ is the modified Bessel function of the first kind of order zero, which is defined by

$$I_0(x) = 1/2\pi \int_0^{2\pi} e^{x\cos\theta}\, d\theta \qquad (4.23)$$

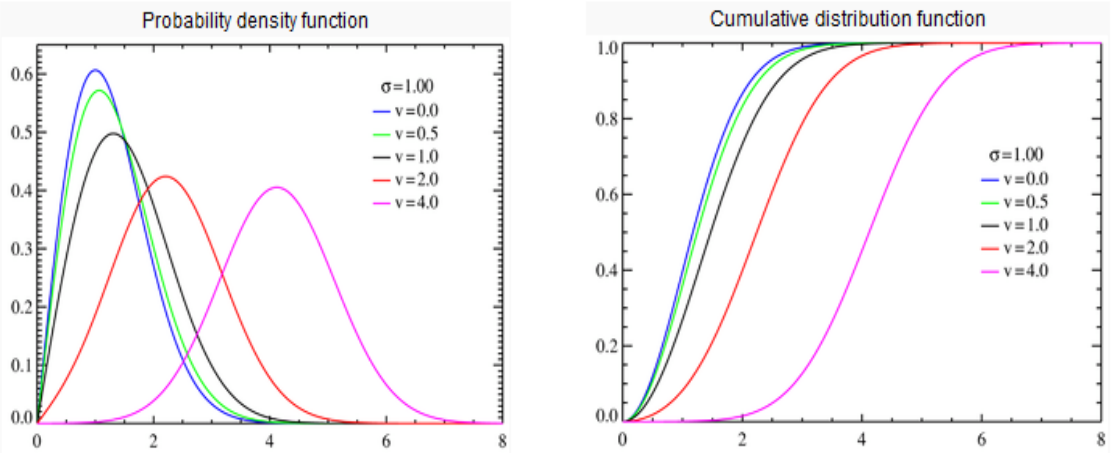

(a) (b)

Figure 4.6 (a) PDF and (b) CDF of Ricean random variable [27]

like the Gaussian random variable, the CDF of a Ricean random variable cannot be written in closed from [28]. The following figure shows the PDF and CDF of Ricean distribution.

4.2.4 Nakagami fading channel

The Nakagami distribution, also known as the “m-distriution” provides greater flexibility in matching experimental data. Nakagami distribution fits in experimental data better than Rayleigh or Rician Distributions.[29]

4.2.4.1 Nakagami-m distribution

The Nakagami distribution or the Nagagami-m distributions a probability distribution related to the gamma distribution. It has two parameters: a shape parameter μ and second parameter controlling spread ω. The fig. 4.7 shows the PDF and CDF of Nakagami-m distribution. [30]

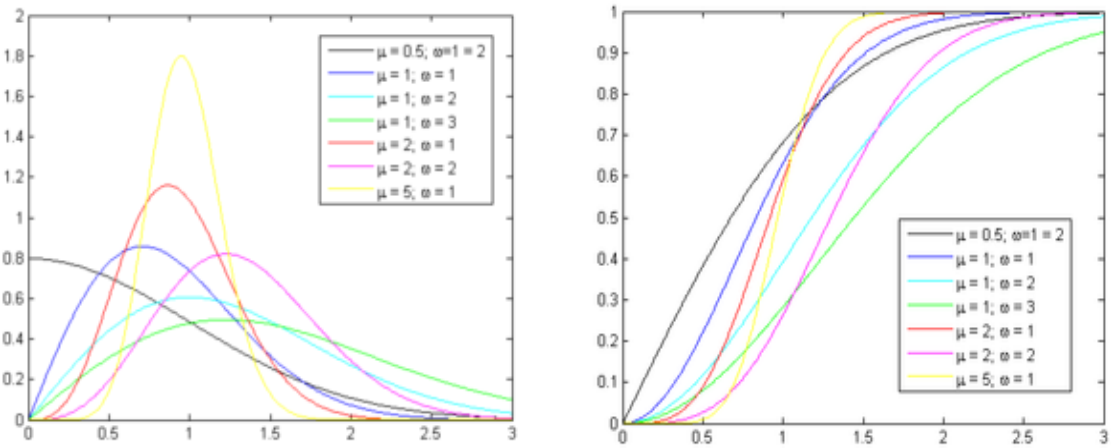

(a) (b)

Figure 4.7: (a) PDF (b) CDF of Nakagami random variable [27]

The Nakagami-m distribution having the PDF of the form

$$f(x;\ \mu, \omega) = \frac{2\mu^{\mu}}{\Gamma(\mu)\omega^{u}} x^{2\mu-1} \exp\left(-\frac{\mu}{\omega}x^{2}\right) \tag{4.24}$$

its CDF is given by

$$f(x;\ \mu, \omega) = P\left(\mu, \frac{\mu}{\omega}\ x^{2}\right) \tag{4.25}$$

in the above equations, the gamma function is a generalization of the factorial function defined by

$$\Gamma(\alpha) = \int_0^{\infty} e^{-t} t^{\alpha-1}\, dt \tag{4.26}$$

where *P* is the incomplete Gama function which is given as

$$P(\alpha, \beta) = \int_0^{\beta} e^{-t} t^{\alpha-1}\, dt \tag{4.27}$$

4.2.4.2 Relation to other random variables

As mentioned earlier, the Nakagami distribution is related to the Gamma distribution. In particular given a random variable Y Gamma (k, θ), it is possible to obtain a random variable X Nakagami (μ, ω), by setting $k = \mu, \theta = {}^{\omega}/_{\theta}$ and taking the square root of Y. [30]

$$X = \sqrt{Y} \tag{4.28}$$

Chapter 5

Results and discussion

In digital transmission, the bit error rate or bit error ratio (BER) is the number of received bits that have been altered due to noise, interference and distortion, divided by the total number of transferred bits during a studied time interval. BER is a unit less performance measure. Mathematically BER can be defined as follows.

$$BER = \frac{Number\ of\ errors}{Total\ Number\ of\ Bits\ transmitted} \tag{5.1}$$

In a communication system, the receiver side BER may be affected by transmission channel noise, interference, distortion, bit synchronization problems, attenuation, wireless multipath fading, etc. The BER may be improved by choosing a strong signal strength (unless this causes cross-talk and more bit errors), by choosing a slow and robust modulation scheme or line coding scheme, and by applying channel coding schemes such as redundant forward error correction codes.

Signal to noise ratio (SNR) is a measure used in science and engineering to quantify how much a signal has been corrupted by noise. It is defined as the ratio of signal power to the noise power corrupting the signal. In less technical terms, SNR compares the level of a desired signal to the level of background noise. The higher the ratio, the less obtrusive the background noise is. SNR is sometimes used informally to refer to the ratio of useful information to false or irrelevant data in a conversation or exchange. The SNR mathematically can be expressed as follows.

$$SNR = 10 \log 10 \left(\frac{Signal\ Power}{Noise\ Power}\right) \tag{5.2}$$

5.1 Performance analysis of 802.11a for different data rates

IEEE 802.11a supports different data rates 6, 12, 18, 24, 36, 48, and 52. Simulation of IEEE 802.11a has been carried out for different data rate in AWGN environment and results are enlisted in this section. From fig. 5.8 and table 5.2, it has been observed, IEEE 802.11a performance keep on degrading with increase in data rate. Loss of 20 dB at BER 10^{-3} has been observed for 52 Mbps data rate compared to 6 Mbps.

Table 5.1: Rate dependent parameters

Data rate (Mbps)	Modulation	Coding rate (R)	Coded bits per subcarrier (N_{BPSC})	Coded bits per OFDM symbol (N_{CBPS})	Data bits per OFDM symbol (N_{DBPS})
6	BPSK	1/2	1	48	24
12	QPSK	1/2	2	96	48
18	QPSK	3/4	2	96	72
24	16-QAM	1/2	4	192	96
36	16-QAM	3/4	4	192	144
48	64-QAM	2/3	6	288	192
54	64-QAM	3/4	6	288	216

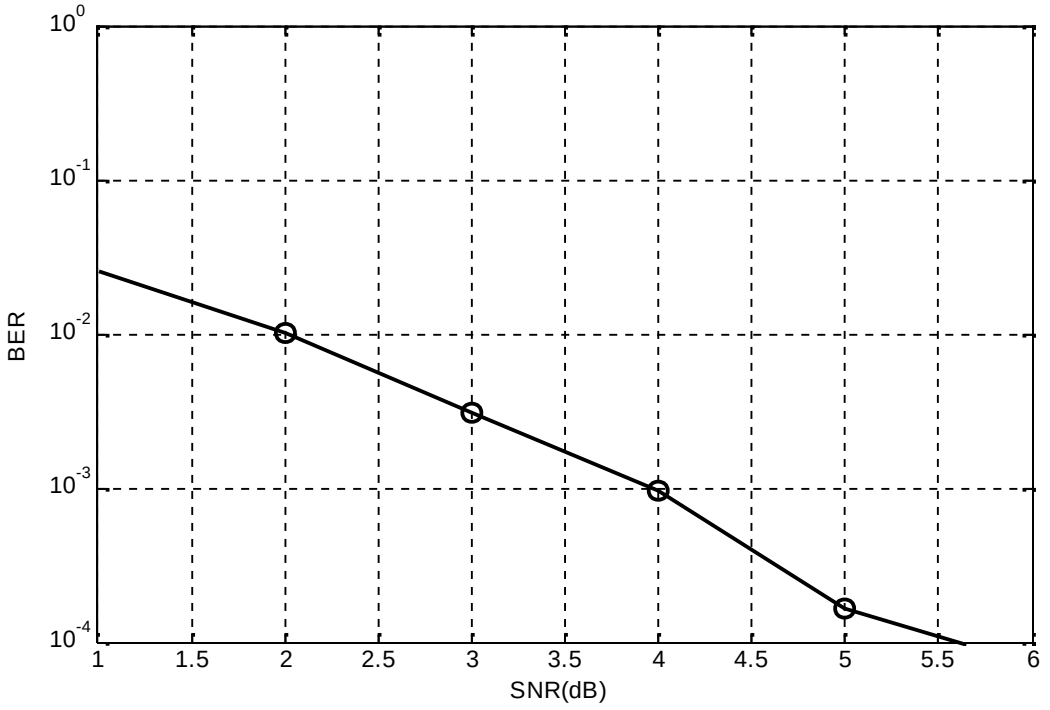

Figure 5.1: BER performance of IEEE 802.11a for 6 Mbps data rate

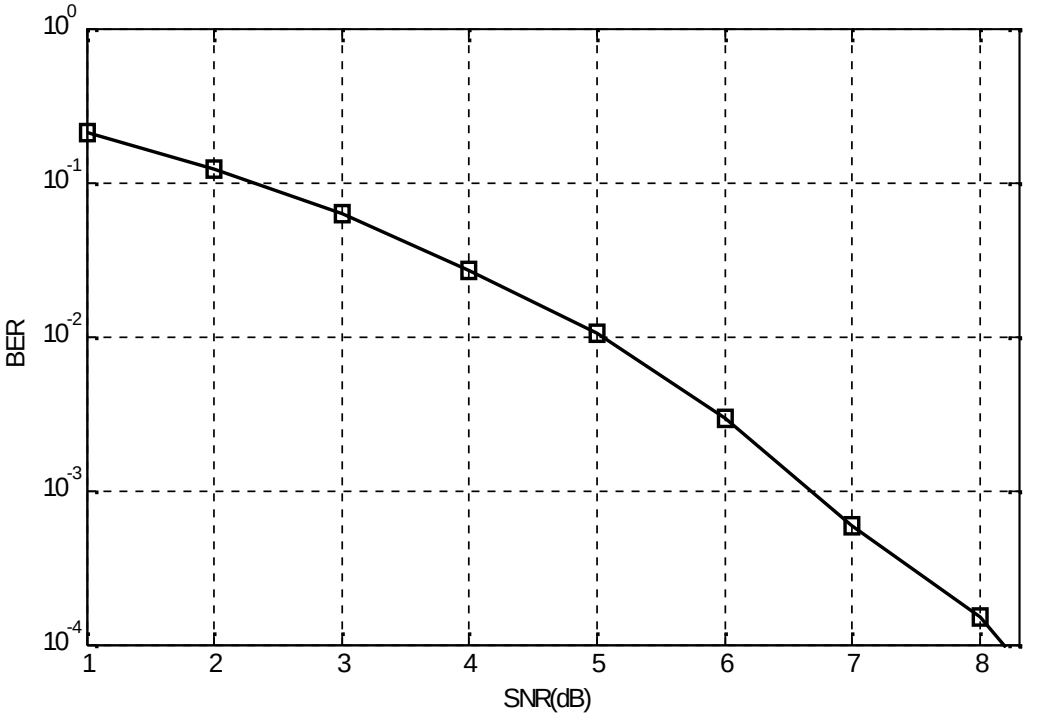

Figure 5.2: BER performance of IEEE 802.11a for 12 Mbps data rate

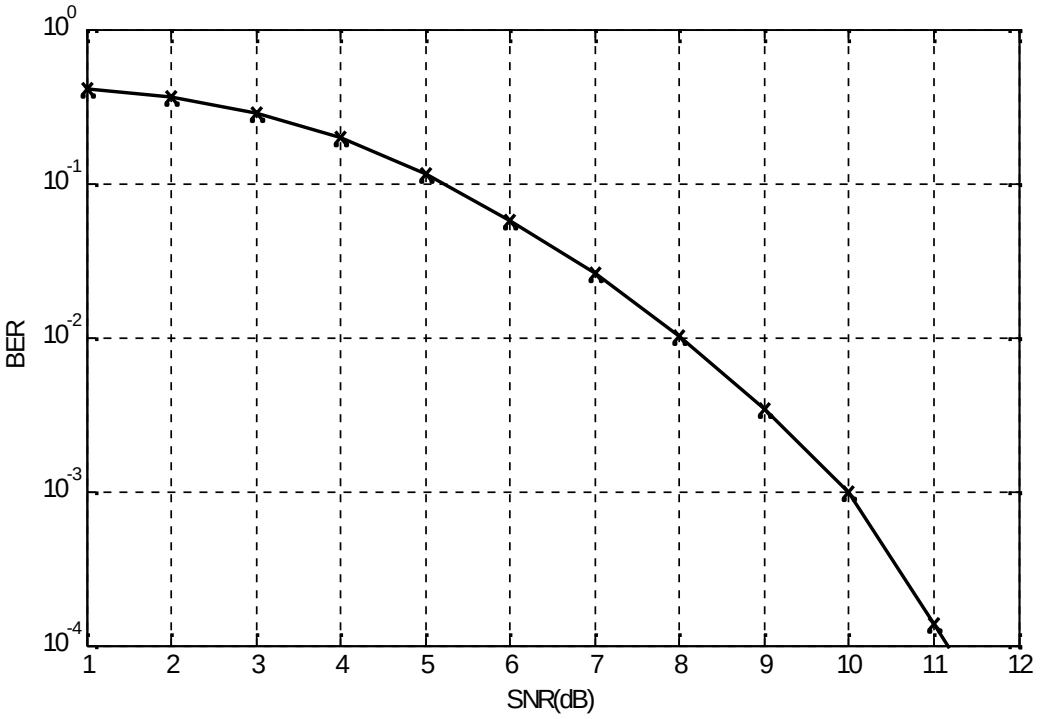

Figure 5.3: BER performance of IEEE 802.11a for 18 Mbps data rate

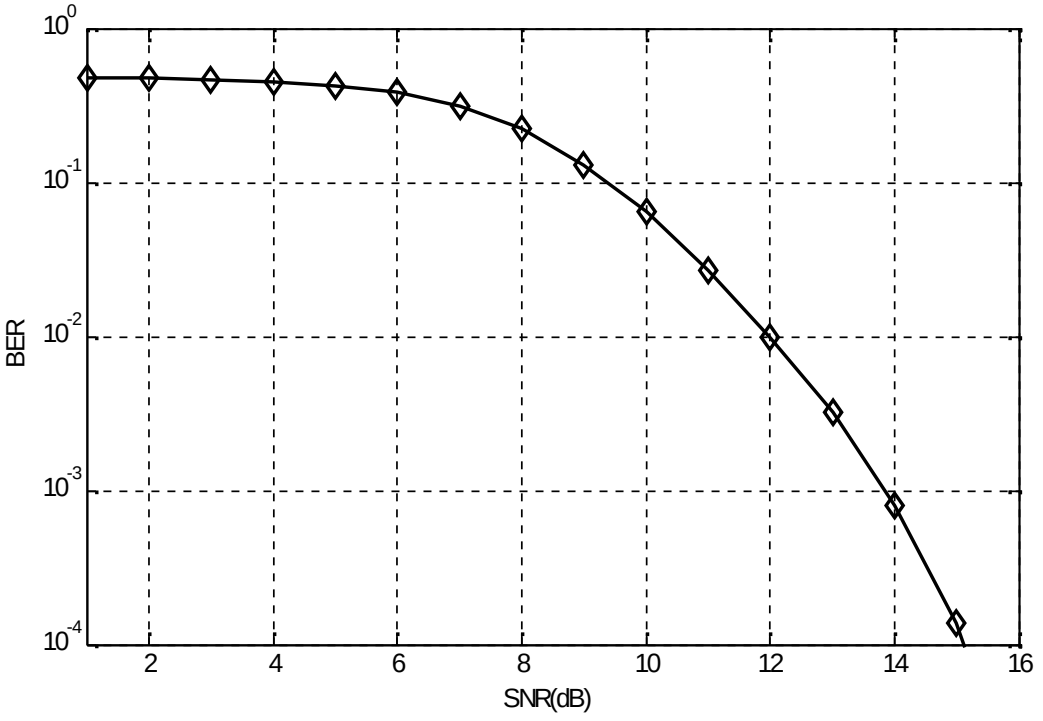

Figure 5.4: BER performance of IEEE 802.11a for 24 Mbps data rate

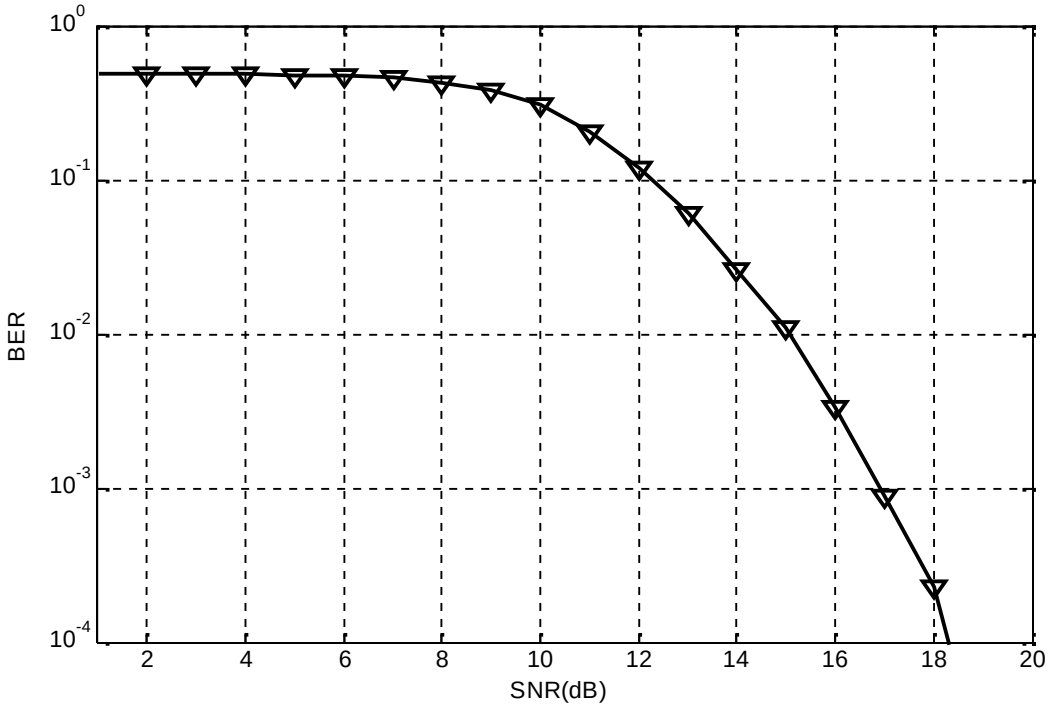

Figure 5.5: BER performance of IEEE 802.11a for 36 Mbps data rate

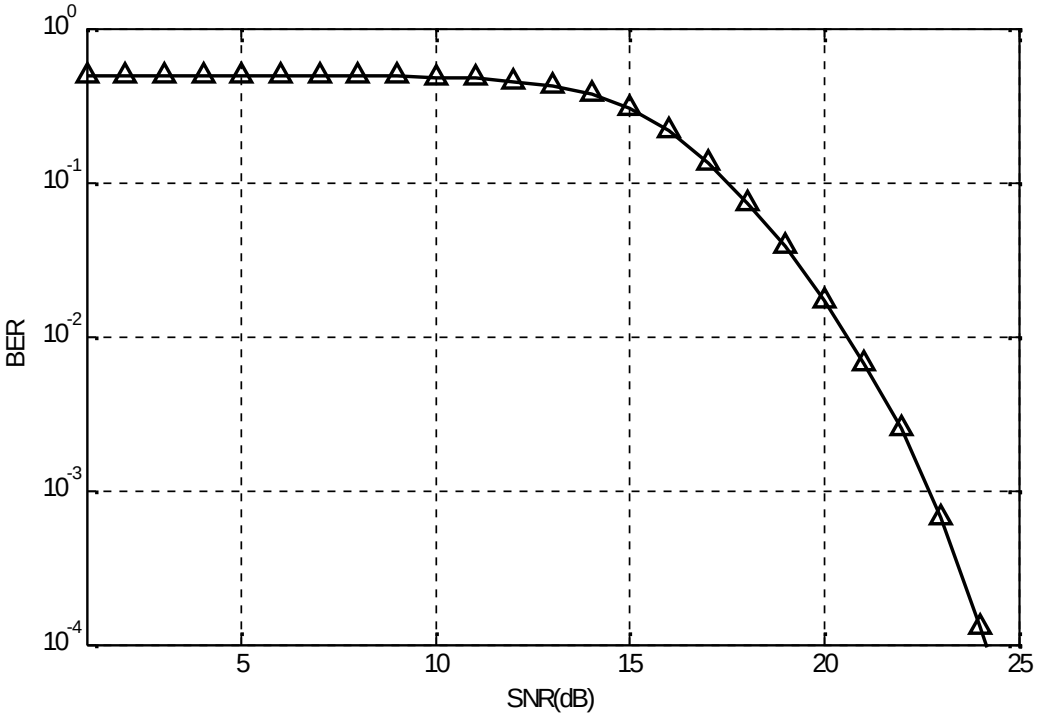

Figure 5.6: BER performance of IEEE 802.11a for 48 Mbps data rate

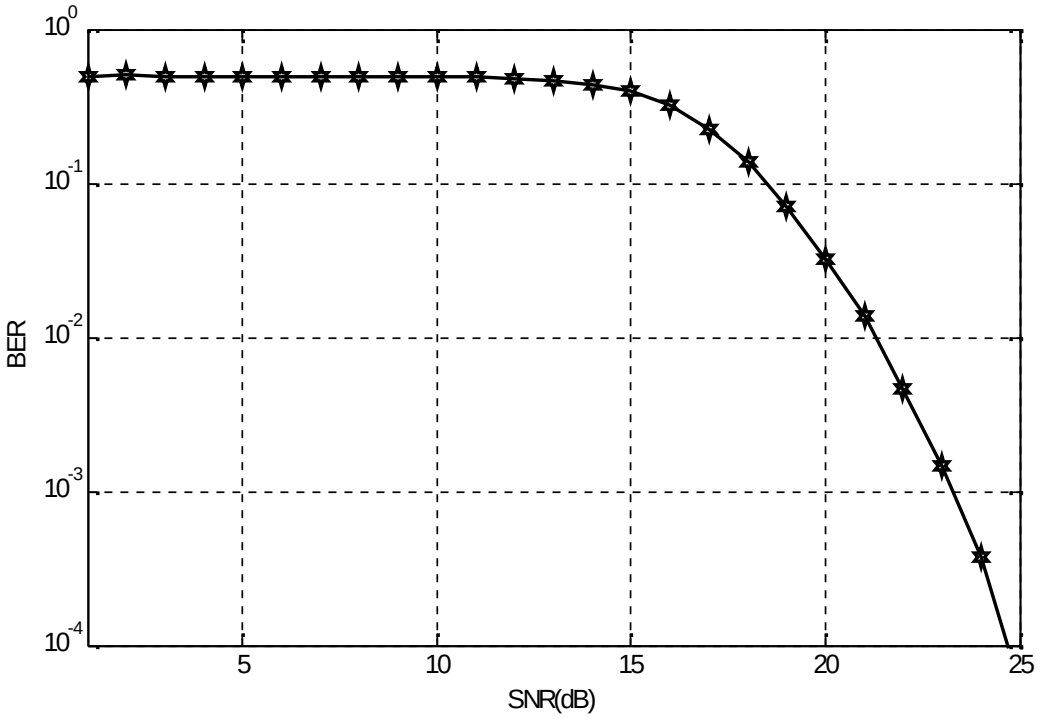

Figure 5.7: BER performance of IEEE 802.11a for 54 Mbps data rate

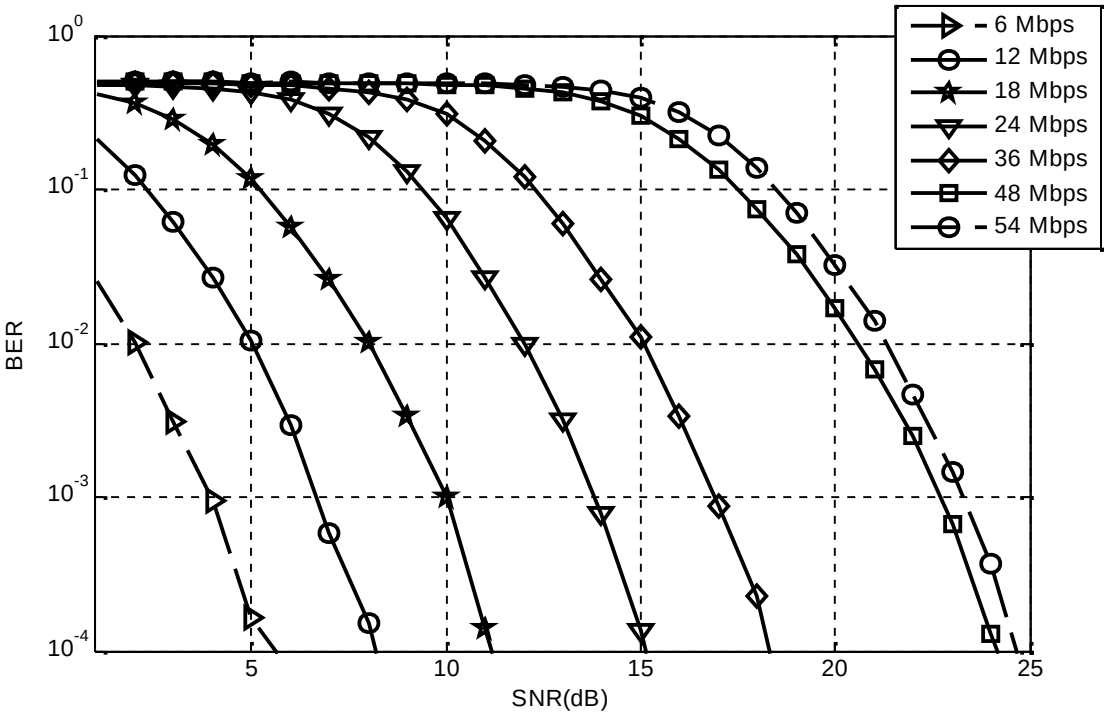

Figure 5.8: BER performance comparison of IEEE 802.11a for different data rate

Table 5.2: BER value for different data rate

SNR(dB)	BER for 6 Mbps	BER for 12 Mbps	BER for 18 Mbps	BER for 24 Mbps	BER for 36 Mbps	BER for 48 Mbps	BER for 54 Mbps
0	0.0257	0.2093	0.4148	0.4798	0.4924	0.4975	0.4976
1	0.0093	0.1213	0.3607	0.4745	0.4909	0.4980	0.4974
2	0.0030	0 .0636	0.2878	0.4649	0.4890	0.4963	0.4977
3	0.0008	0.0273	0.1983	0.4489	0.4852	0.4961	0.4965
4	0.0002	0.0101	0.1155	0.4220	0.4793	0.4968	0.4970
5	0	0.0030	0.0569	0.3830	0.4712	0.4949	0.4971
6	0	0.0008	0.0259	0.3087	0.4574	0.4938	0.4956
7	0	0.0001	0.0099	0.2212	0.4300	0.4909	0.4948
8	0	0	0.0035	0.1296	0.3838	0.4882	0.4933
9	0	0	0.0009	0.0631	0.3062	0.4816	0.4921
10	0	0	0	0.0271	.2099	.4721	.4879
11	0	0	0	0.0101	0.1215	0.4545	0.4811
12	0	0	0	0.0030	0.0600	0.4244	0.4679
13	0	0	0	0.0008	0.0265	0.3771	0.4433
14	0	0	0	0.0002	0.0104	0.3051	0.3941
15	0	0	0	0	0.0034	0.2159	0.3190
16	0	0	0	0	0.0007	0.1355	0.2213
17	0	0	0	0	0.0002	0.0750	0.1361
18	0	0	0	0	0	0.0382	0.0707
19	0	0	0	0	0	0.0173	0.0326
20	0	0	0	0	0	0.0068	0.0136
21	0	0	0	0	0	0.0023	0.0042
22	0	0	0	0	0	0.0007	0.0013
23	0	0	0	0	0	.00002	0.0013
24	0	0	0	0	0	0	0.0004
25	0	0	0	0	0	0	0.0001

5.2 Performance of IEEE 802.11a for different channels

A Convolution codes with code rate 1/2 has been used. The mapping schemes used for simulation is QPSK. In this section IEEE 802.11a has been simulated in different environment, AWGN, Rayleigh fading, Ricean fading and Nakagami fading. Nakagami fading with, shaping factor $(\mu) = 0.5$ is used. This is the worst channel condition in wireless communication.

From fig. 5.13 and table 5.3, it has been observed, there is 4 dB of loss at BER 10^{-3} for Rayleigh fading channel as compared to Ricean fading channel. For Nakagami fading channel, loss of 20 dB has been observed with compared to Rayleigh fading channel at same BER.

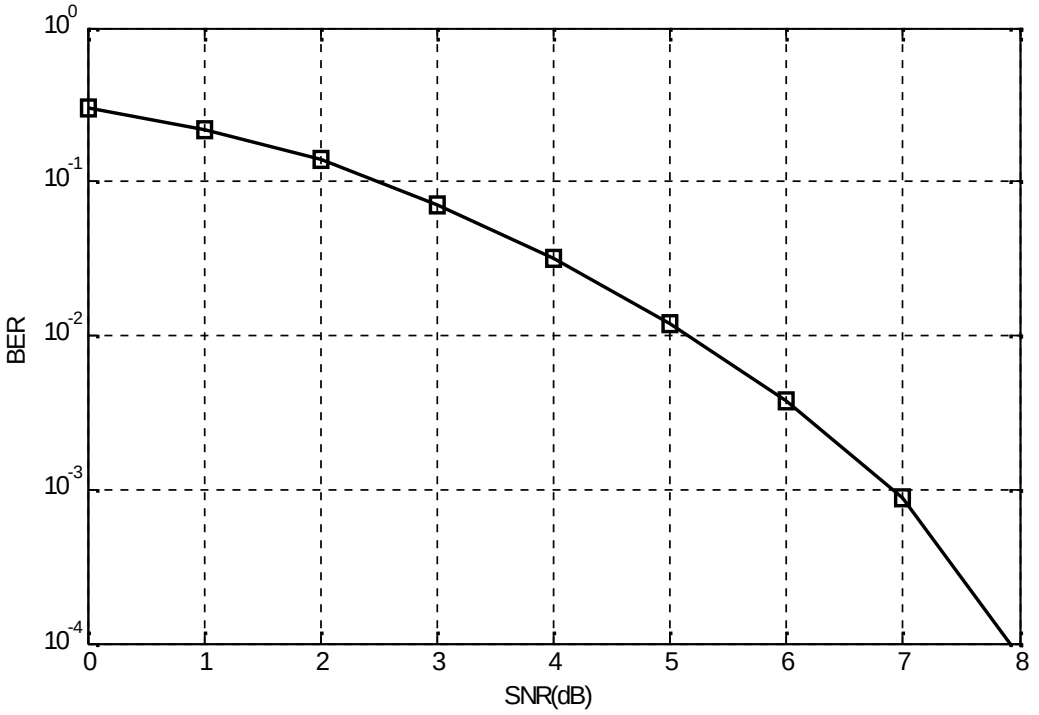

Figure 5.9: BER performance of IEEE 802.11a over AWGN channel

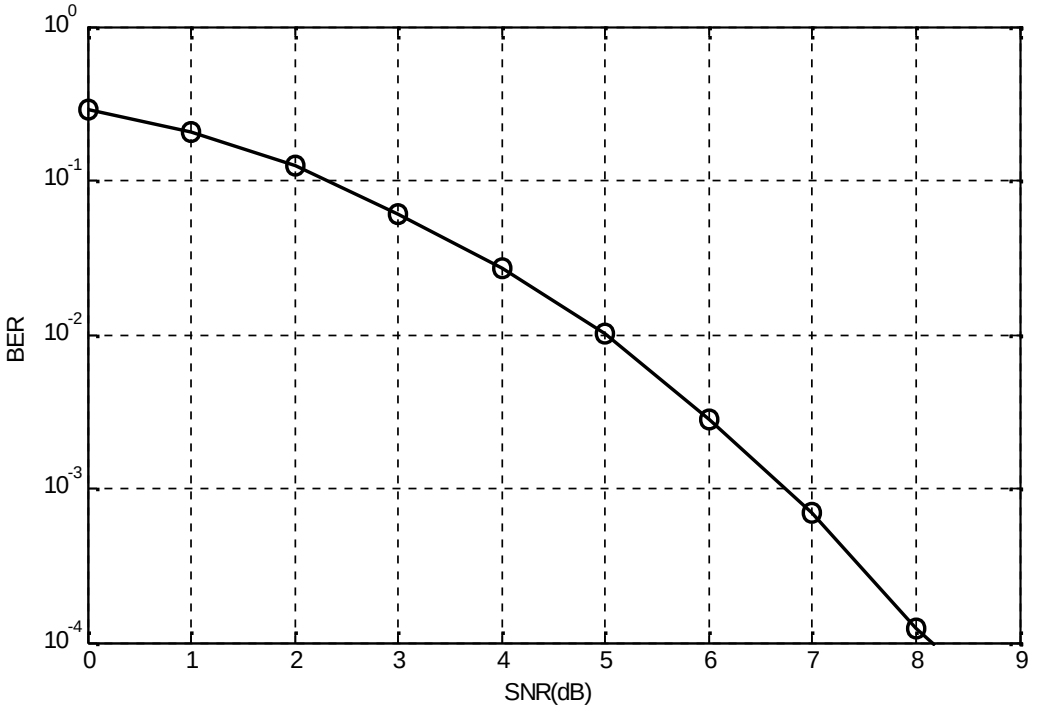

Figure 5.10: BER performance of IEEE 802.11a over Ricean fading channel

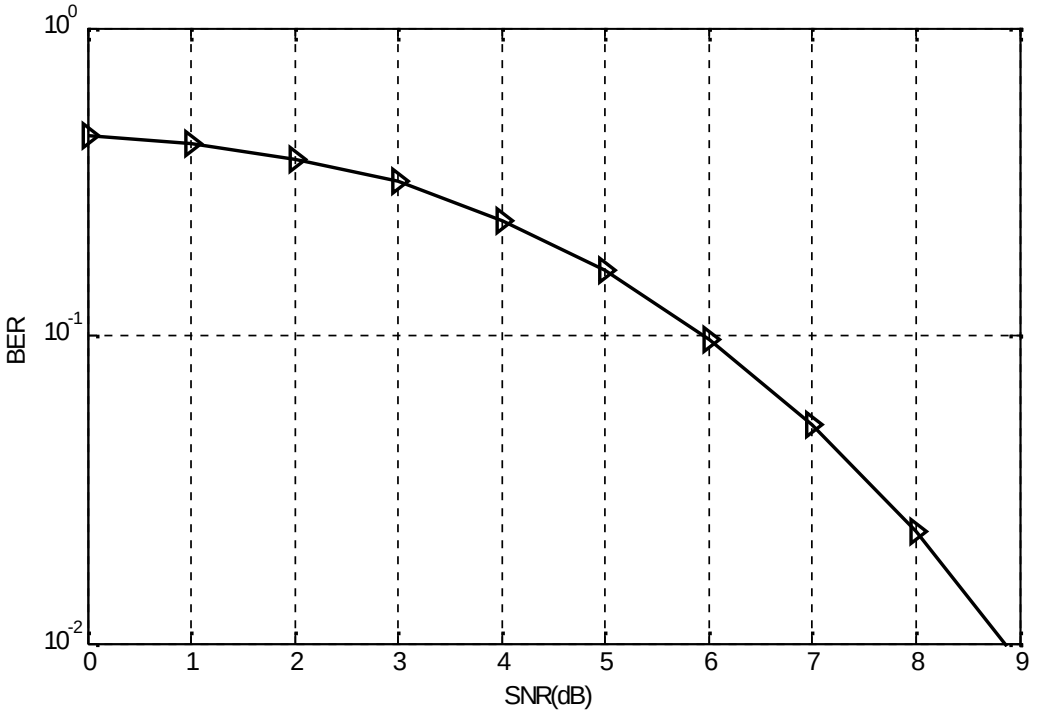

Figure 5.11: BER performance of IEEE 802.11a over Rayleigh fading channel

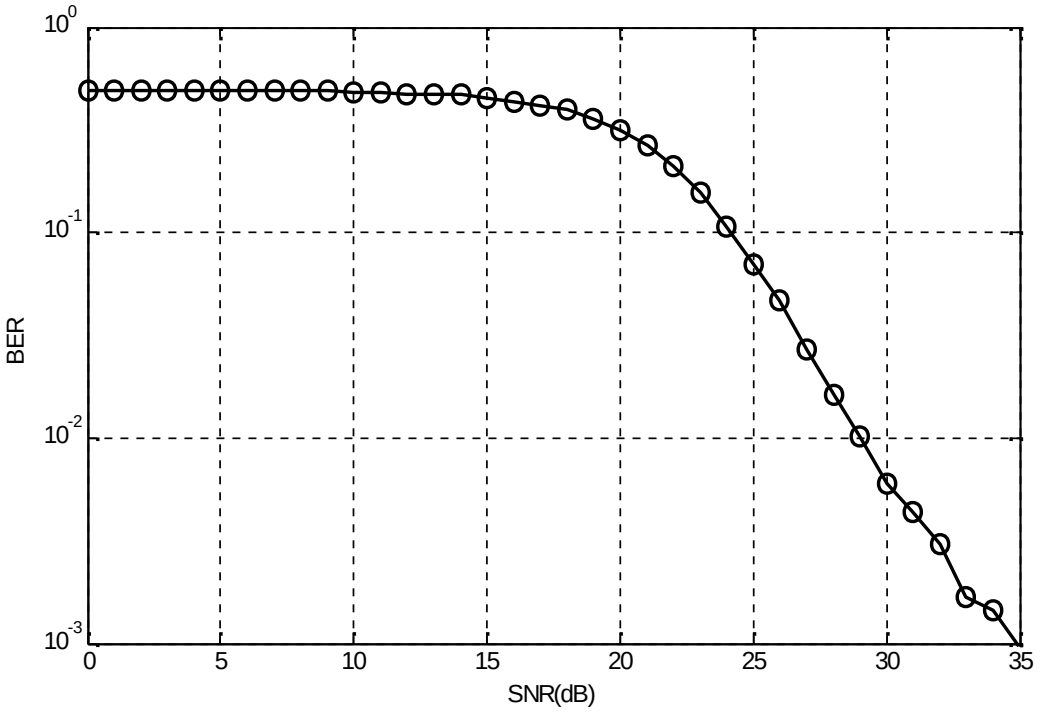

Figure 5.12: BER performance of IEEE 802.11a over Nakagami fading channel

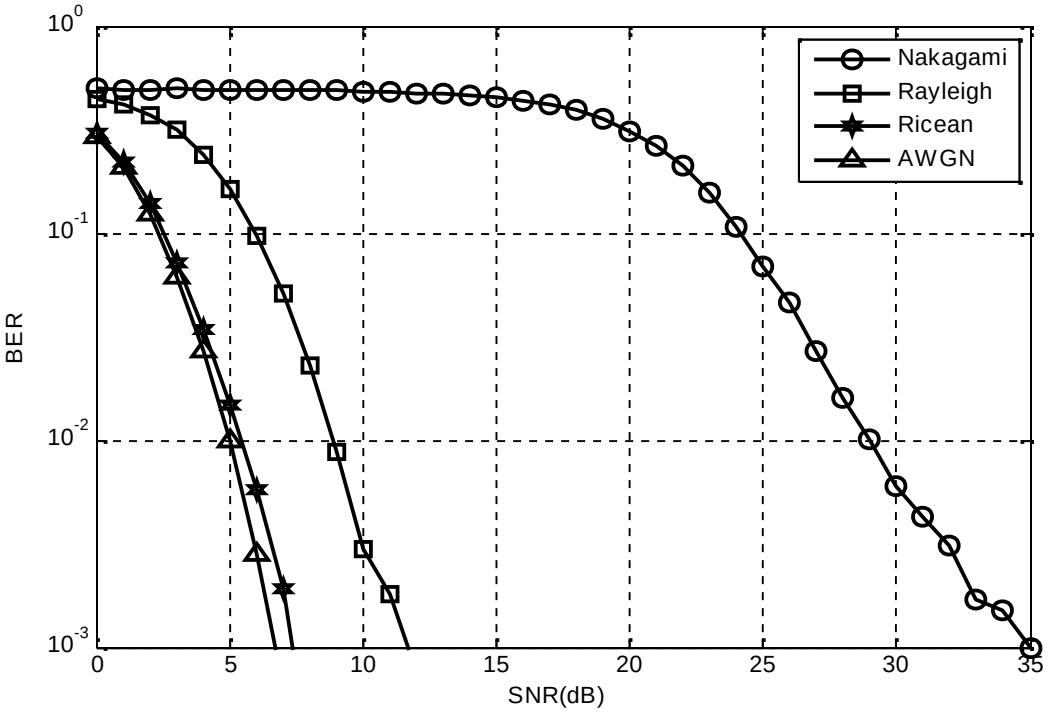

Figure 5.13: BER performance Comparison of IEEE 802.11a for different channels

Table 5.3: BER value for different channels

SNR (dB)	Nakagami fading channel with $\mu = 0.5$	Rayleigh fading channel	Ricean fading channel	AWGN channel
0	0.4967	0.4434	0.3051	0.2899
1	0.4941	0.4180	0.2204	0.2082
2	0.4959	0.3732	0.1385	0.1245
3	0.4965	0.3187	0.0711	0.0613
4	0.4937	0.2376	0.0314	0.0271
5	0.4945	0.1640	0.0118	0.0100
6	0.4937	0.0967	0.0038	0.0028
7	0.4869	0.0513	0.0009	0.0007
8	0.4897	0.0230	0.0001	0.0001
10	0.4871	0.0088	0.0000	0.0000
11	0.4827	.0030	0	0
12	0.4820	.0018	0	0
13	0.4745	.0008	0	0
14	0.4717	.0001 0	0	0
15	0.4668	.00001	0	0

.

5.3 Performance of IEEE 802.11a for Different Doppler shifts

A Convolution code with code rate 1/2 has been used. The mapping schemes used for simulation is QPSK. For the simulation purpose Rayleigh channel with two paths and delay spread of 0.2 μsec is used. From fig. 5.17 and table 5.4, it has been observed that BER performance of IEEE 802.11a degrades with increase in Doppler shift. Loss of 3.5 dB at BER 10^{-3} has been observed at 500 Hz Doppler shift as compared to 100 Hz.

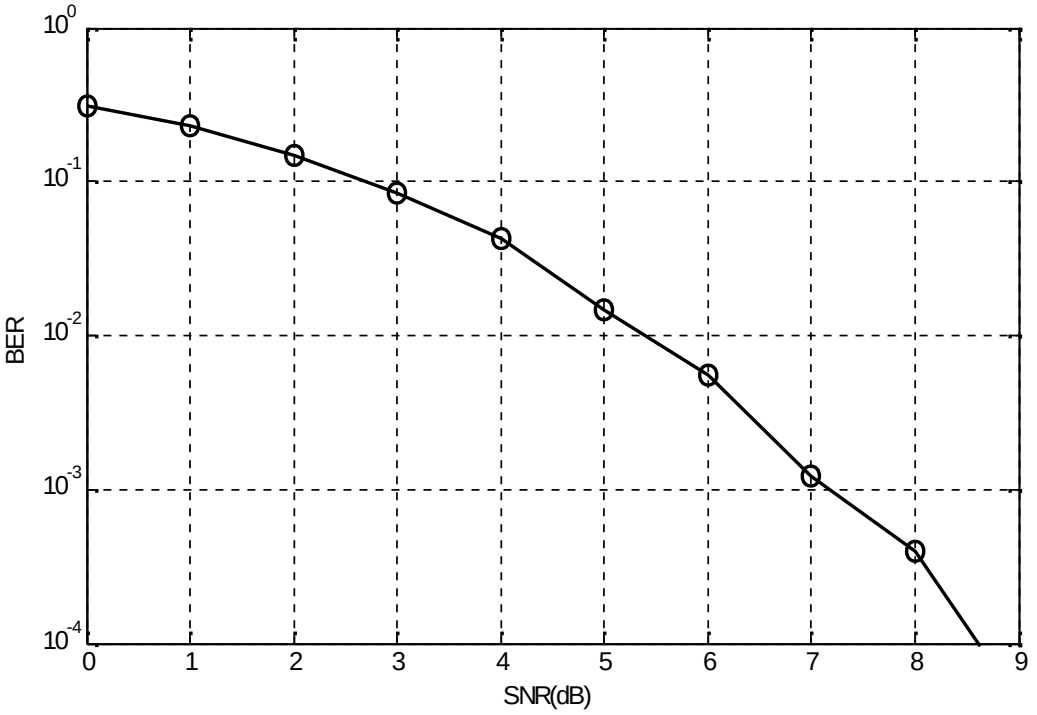

Figure 5.14: BER performance of IEEE 802.11a for 100 Hz Doppler shifts

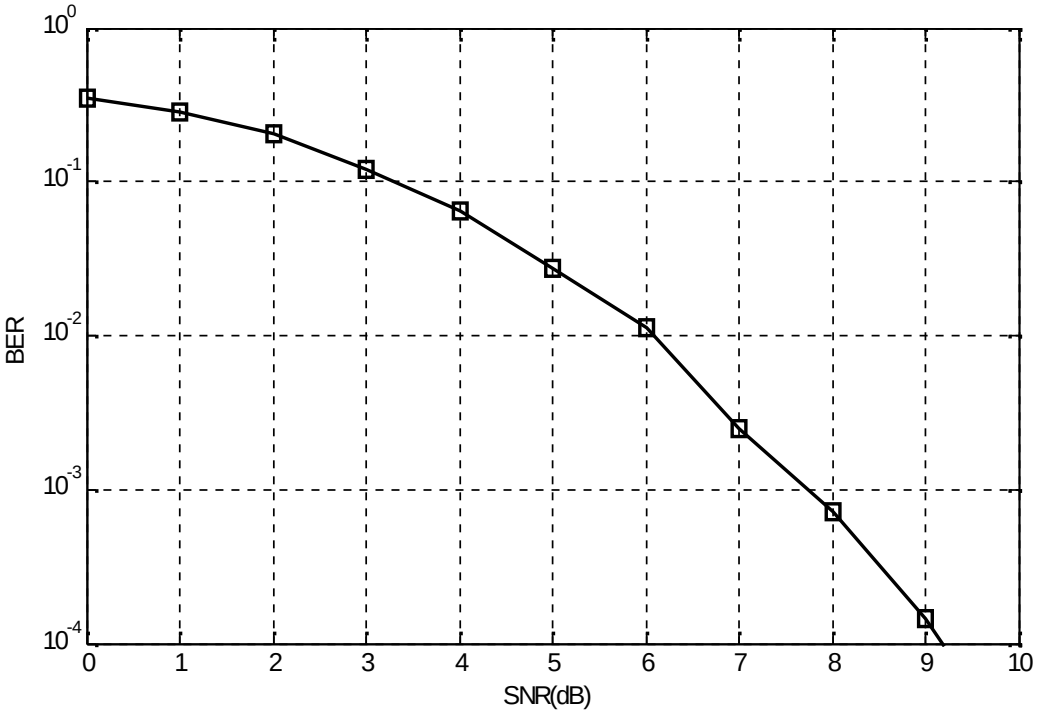

Figure 5.15: BER performance of IEEE 802.11a for 200Hz Doppler shifts

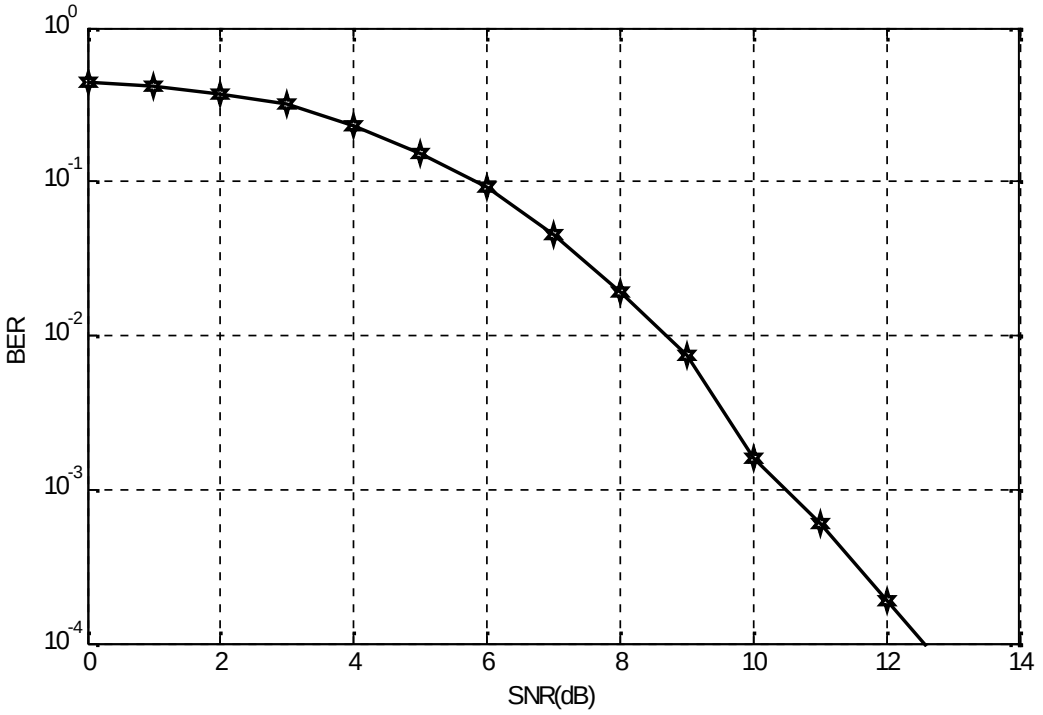

Figure 5.16: BER performance of IEEE 802.11a for 500Hz Doppler shifts

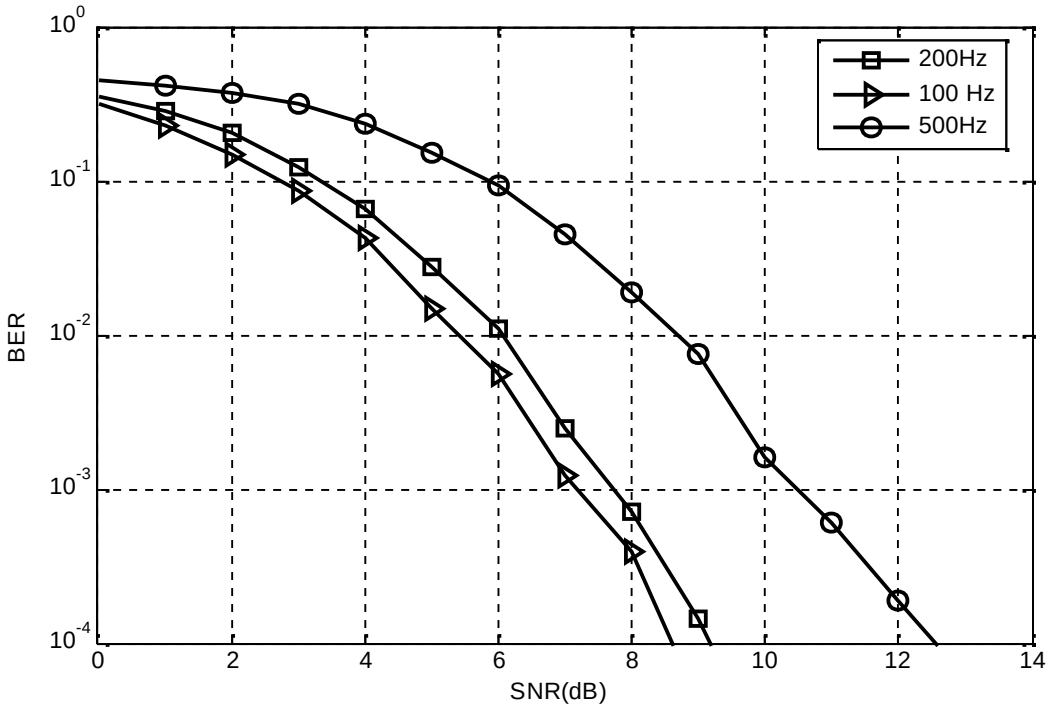

Figure 5.17: BER performance comparison of IEEE 802.11a for different Doppler shifts

Table 5.4: BER value for different Doppler shift

SNR(dB)	BER for 100 Hz	BER for 200 Hz	BER for 200 Hz
0	0.3130	0.3533	0.4489
1	0.2311	0.2871	0.4116
2	0.1483	0.2024	0.3154
3	0.0854	0.1219	0.2318
4	0.0427	0.0650	0.1531
5	0.0149	0.0274	0.0922
6	0.0056	0.0111	0.0448
7	0.0012	0.0025	0.0191
8	0.0004	0.0007	0.0075
9	0	0.0001	0.0016
10	0	0	0.0006
11	0	0	0.0002
12	0	0	0.0001

5.4 Effect of CP Length in the Performance of IEEE 802.11a

Radio channels are time dispersive in nature, which may cause interference between two conjugative symbols. This phenomena is regarded as inter symbol interference. Because of this the system performance may degrade. But in OFDM based system ISI could be overcome by using CP. The effect of CP in performance of IEEE 802.11a is analysed in this section. Different CP length used for simulation are CP= 0 μsec, CP= 0.4 μsec and CP= 0.8 μsec.

A Convolution codes with code rate 1/2 has been used. The mapping schemes used for simulation is QPSK. For the simulation purpose Rayleigh channel with three different paths and delay spread of 0.2 μsec is used. From table 5.5 and fig.5.21, it has been observed, system gain increases with increase in CP duration. Gain of 5 dB at BER 10^{-3} has been observed with CP of 0.8 μse compared to with out CP.

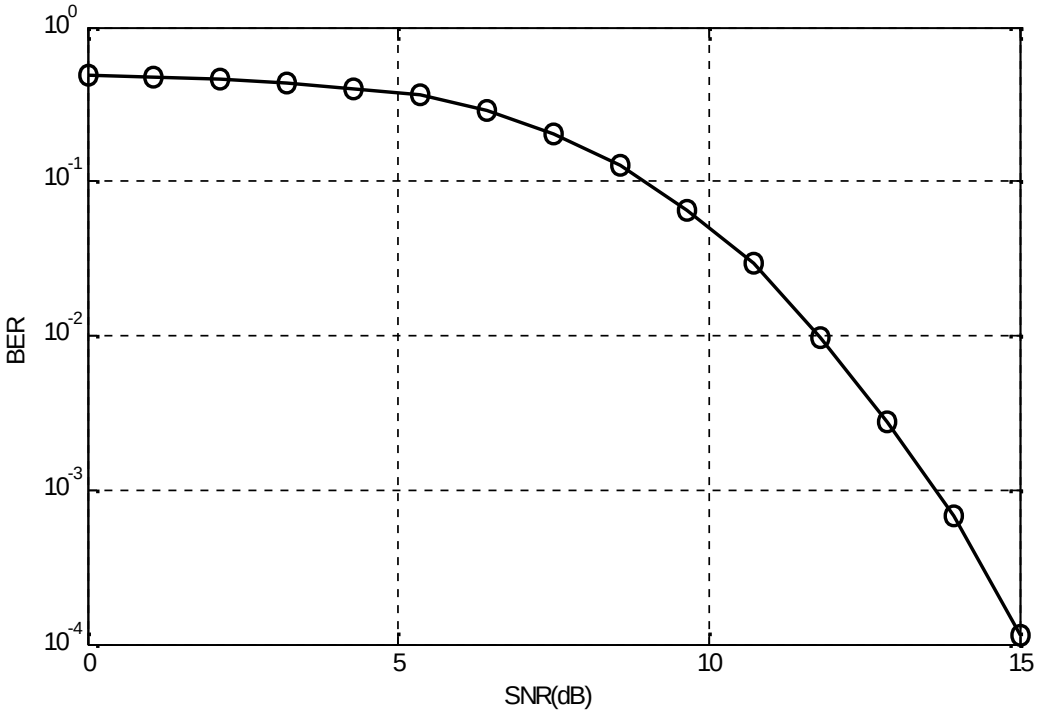

Figure 5.18: BER performance of IEEE 802.11a without CP

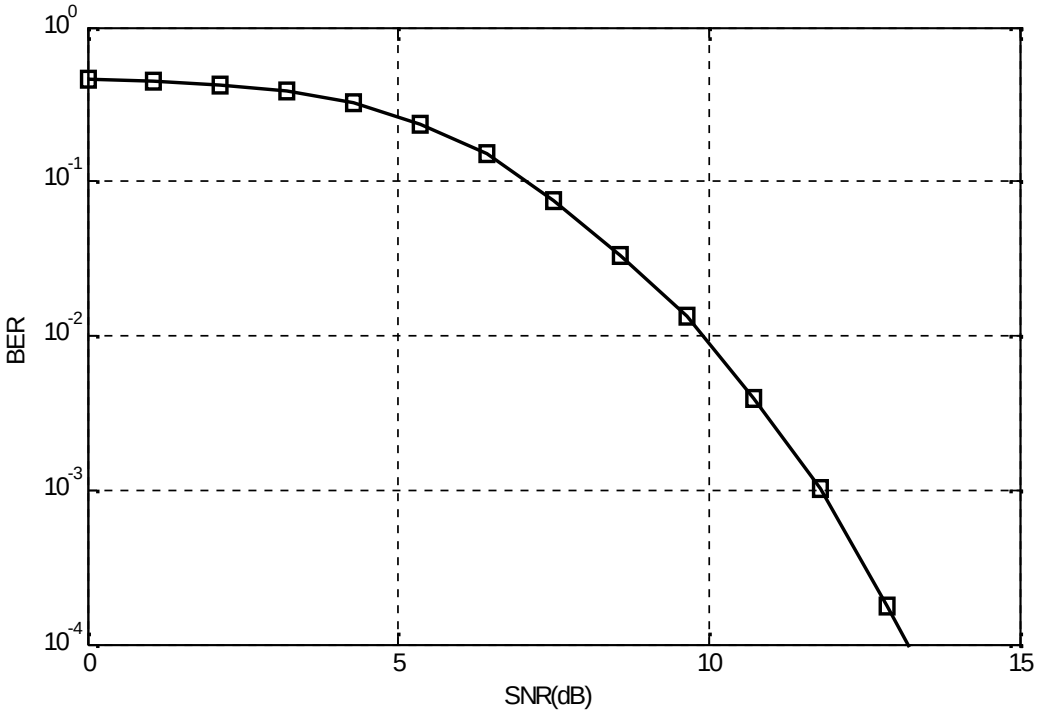

Figure 5.19: BER performance of IEEE 802.11a with 0.4 μsec CP

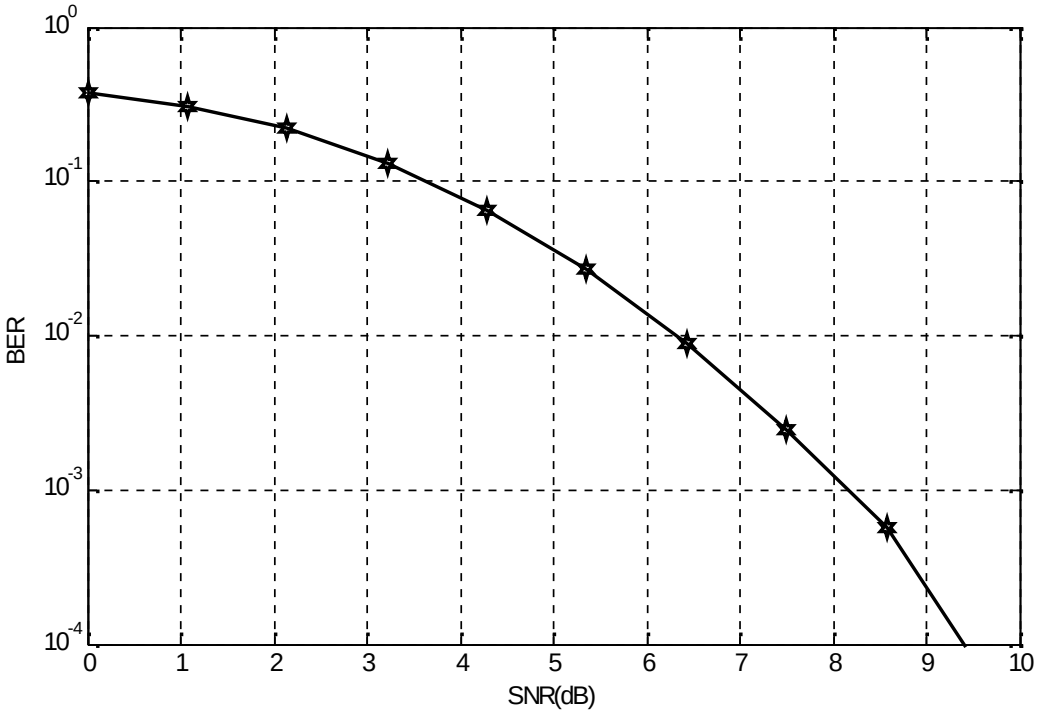

Figure 5.20: BER performance of IEEE 802.11a with 0.8 μsec CP

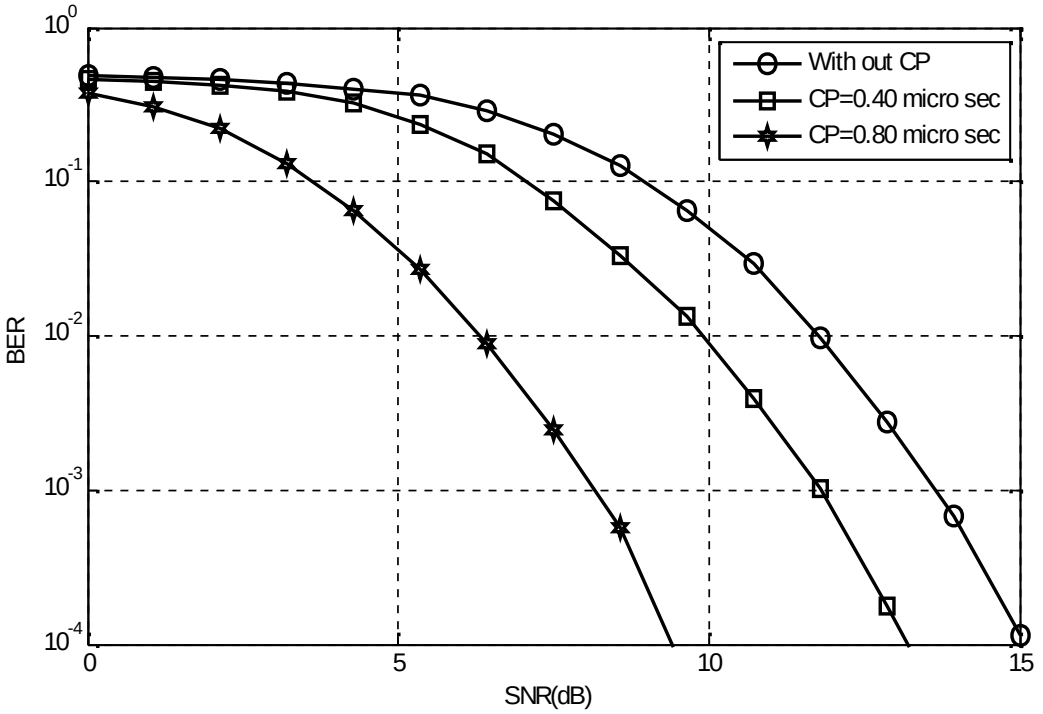

Figure 5.21: BER performance of IEE 802.11a for different CP

Table 5.5: BER value for different CP

SNR(dB)	Without CP	CP=0.4μsec	CP=0.8 μsec
0	0.4836	0.4647	0.3781
1	0.4724	0.4140	0.3047
2	0.4563	0.3804	0.2184
3	0.4375	0.323	0.1257
4	0.4060	0.2341	0.0620
5	0.3619	0.1486	0.0255
6	0.2801	0.0761	0.0092
7	0.2079	0.0293	0.0023
8	0.1301	0.0037	0.0006
9	0.0666	0.0015	0.0001
10	0.0316	0.0003	0
11	0.0109	0	0
12	0.0022	0.0000	0
13	0.0007	0	0
14	0.0001	0	0

5.5 Performance Analysis of 802.11a for Different FEC

Convolution and RS codes with code rate 1/2 have been used. The mapping schemes used for simulation is QPSK. Fig. 5.25 shows the BER comparison of IEEE 802.11a in Rayleigh fading environment. From fig. 5.25 and table 5.6 it has been observed, in presence of FEC. 802.11a performance is better than without FEC. There is 3 dB of gain at BER 10^{-3} with CC and gain 4 dB with RS. This shows that RS coding has gain of 1 dB as compared to CC.

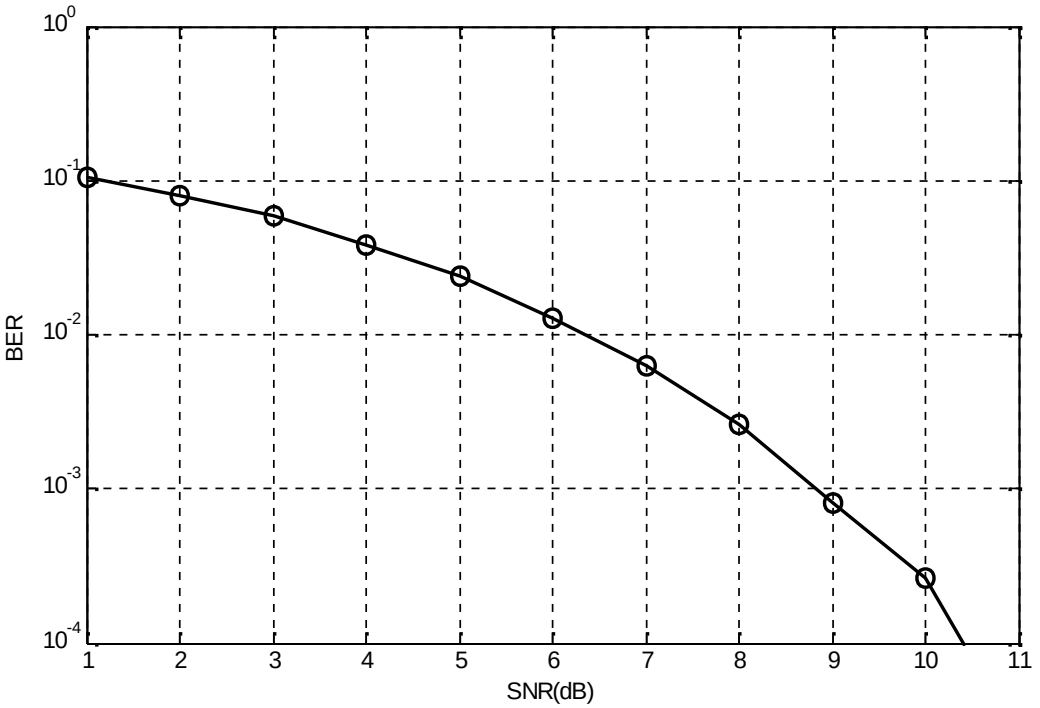

Figure 5.22: BER performance of IEEE 802.11a without FEC

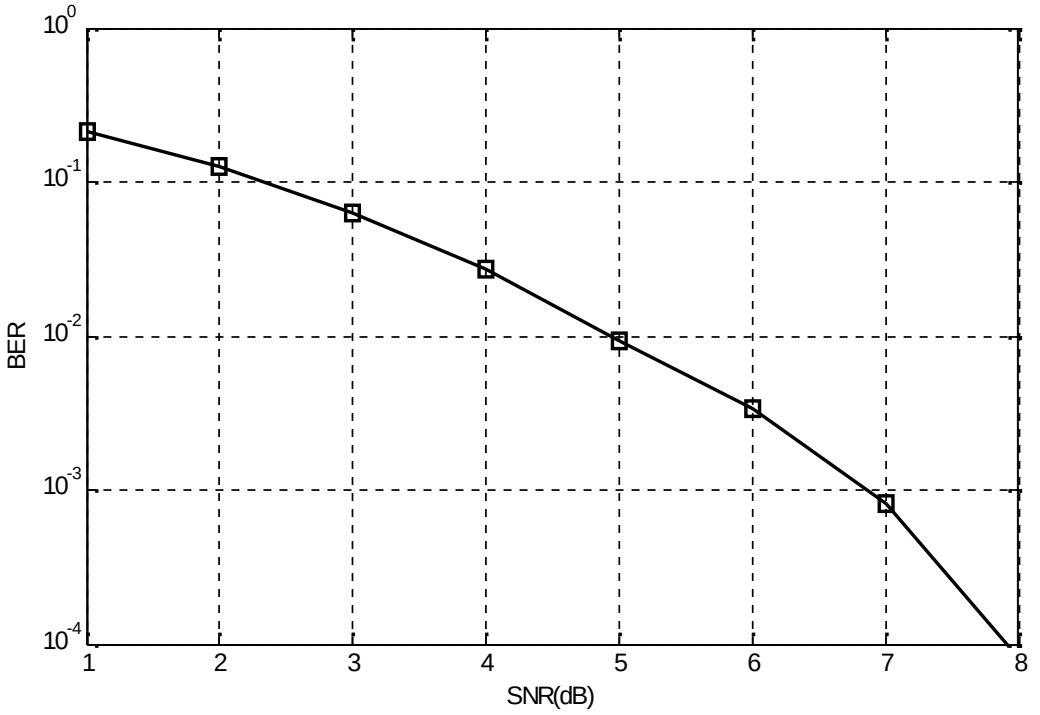

Figure 5.23: BER performance of IEEE 802.11a with CC

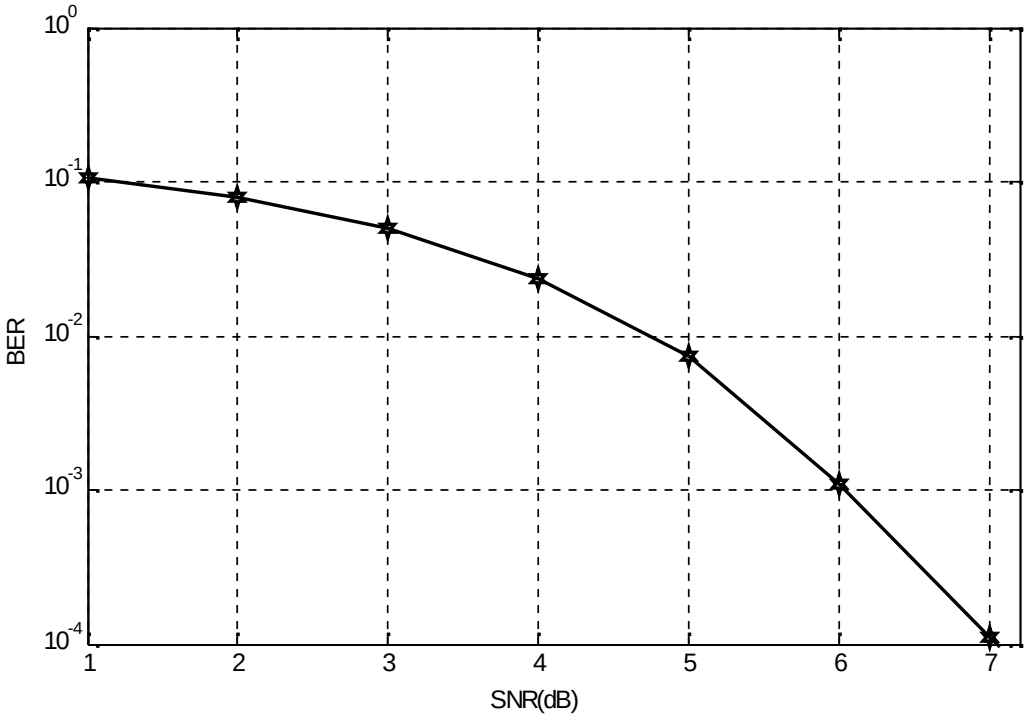

Figure 5.24: BER performance of IEEE 802.11a with Rs code

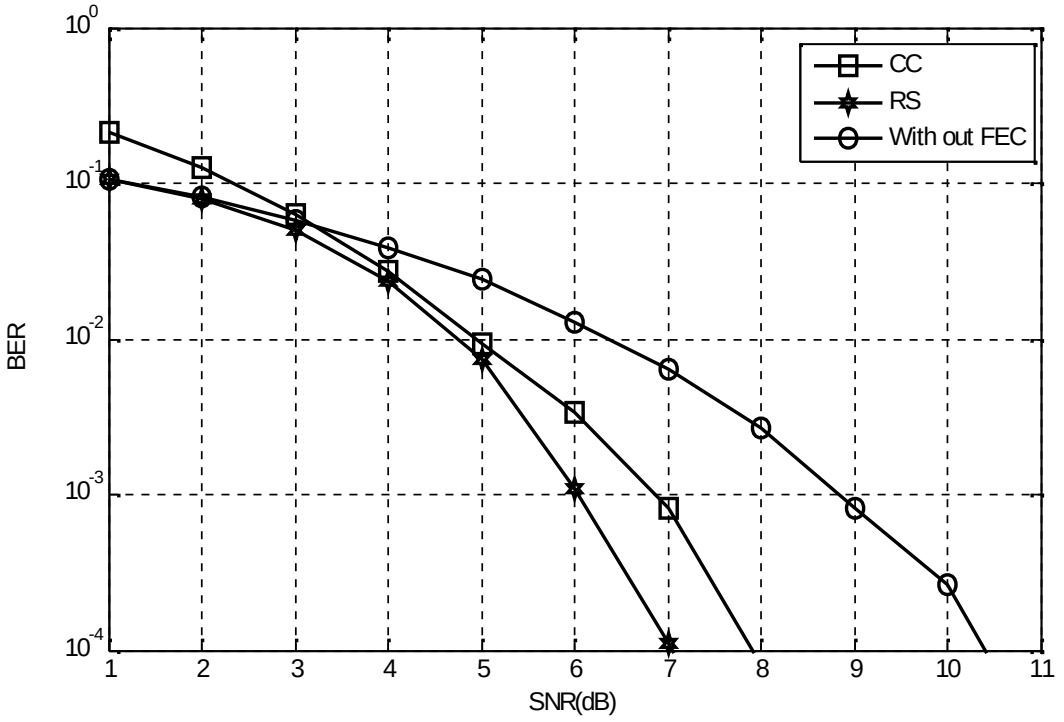

Figure 5.25: BER performance comparison of IEEE 802.11a for different FEC

Table 5.6: Value of BER for different FEC

SNR(dB)	BER for CC	BER for RS	Without coding
0	0.2095	0.1061	0.1060
1	0.1260	0.0782	0.0805
2	0.0623	0.0495	0.0583
3	0.0275	0.0236	0.0381
4	0.0093	0.0074	0.0239
5	0.0033	0.0011	0.0129
6	0.0008	0.0001	0.0064
7	0.0001	0.0000	0.0027
8	0.0000	0.0000	0.0008
9	0.0000	0.0000	0.0003

5.6 PAPR Analysis and Reduction Using SLM Technique

A Convolution codes with code rate 1/2 has been used. The mapping schemes used for simulation is QPSK. WLAN 802.11a is OFDM based system, so it has to deal with PAPR problem. The simulation for PAPR has been carried out using 5000 symbols.

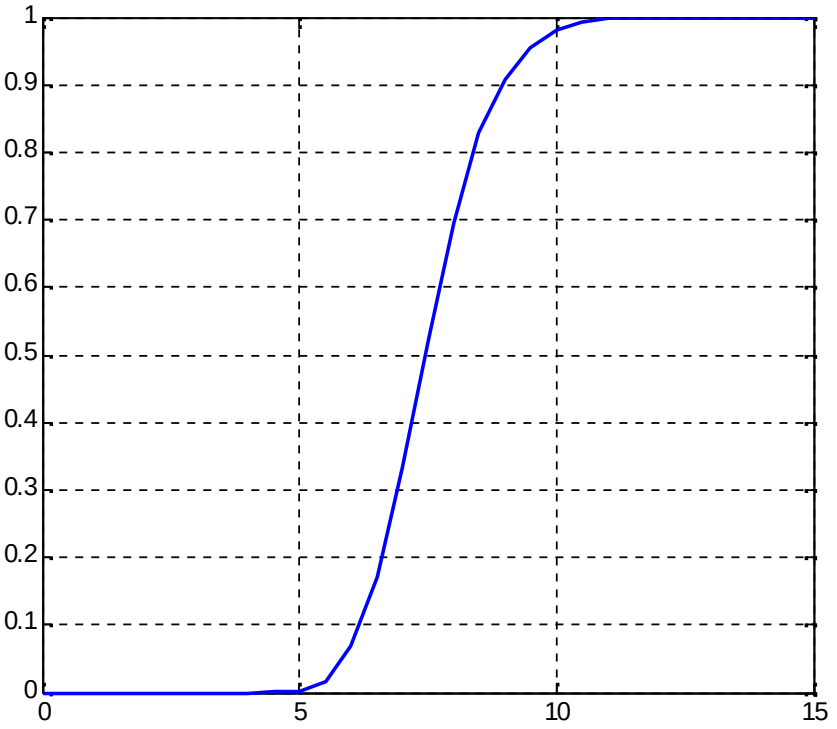

Figure 5.26: CCDF function for PAPR

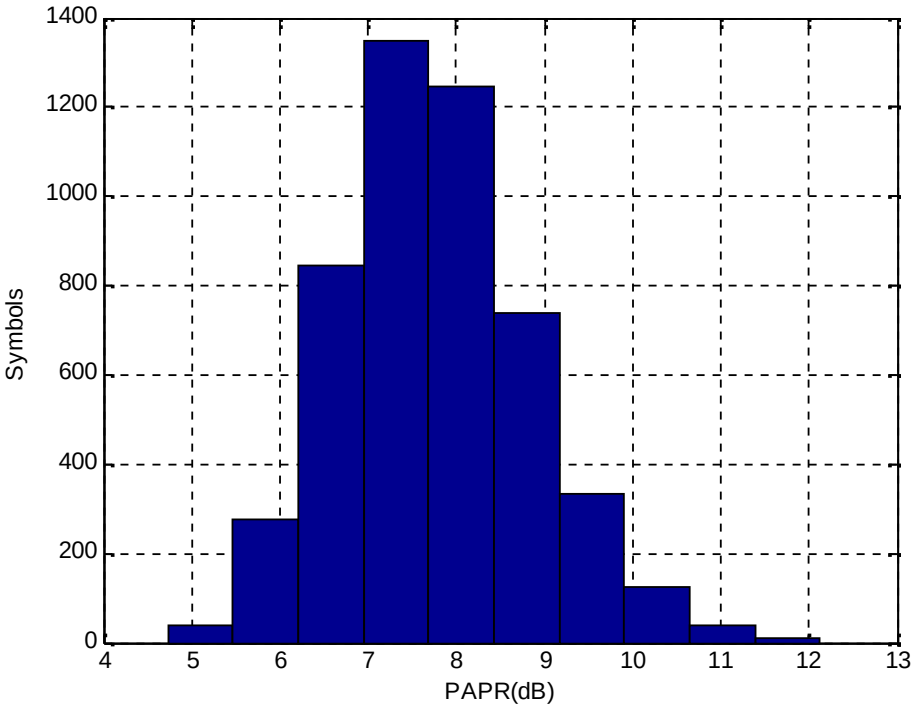

Figure 5.27: Histogram for PAPR

About 12.2 dB PAPR for IEEE 802.11a has been observed, with elapsed time of 19.95 sec.

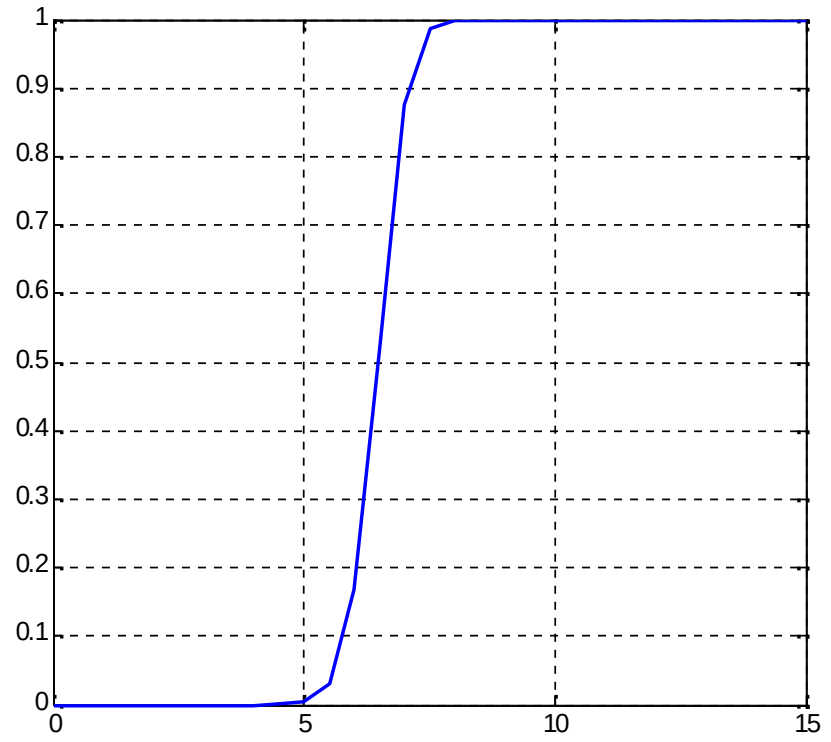

Figure 5.28: CCDF function for PAPR after applying SLM with U=10

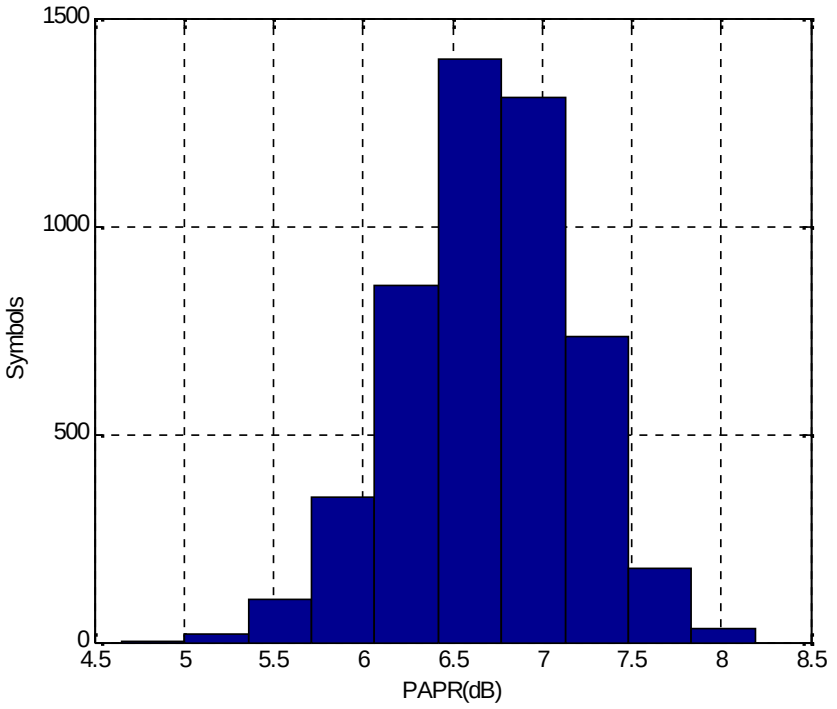

Figure 5.29: Histogram for PAPR after applying SLM with U=10

About 4 dB PAPR has been reduces by using 10 different phase sequence.

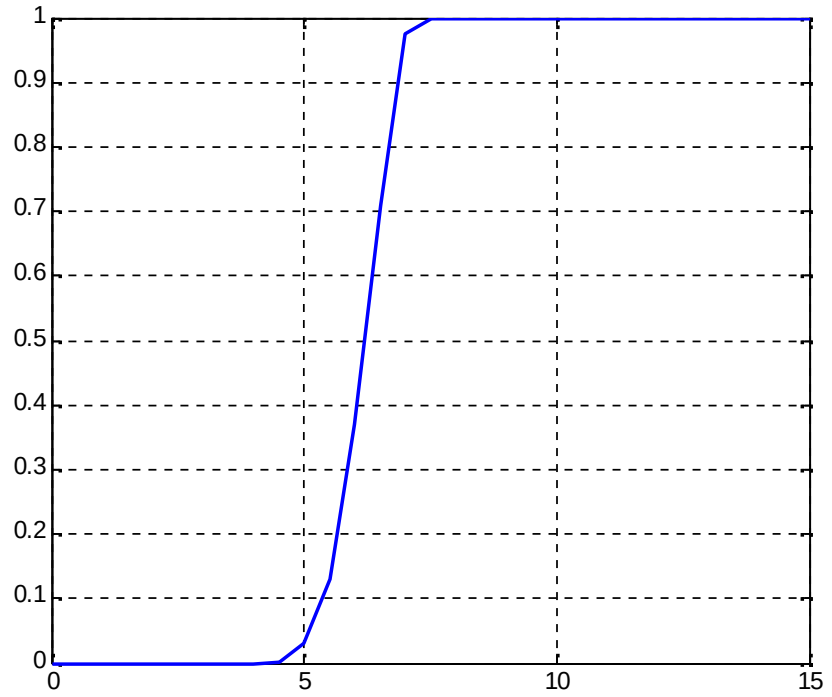

Figure 5.30: CCDF function for PAPR after applying SLM with U=20

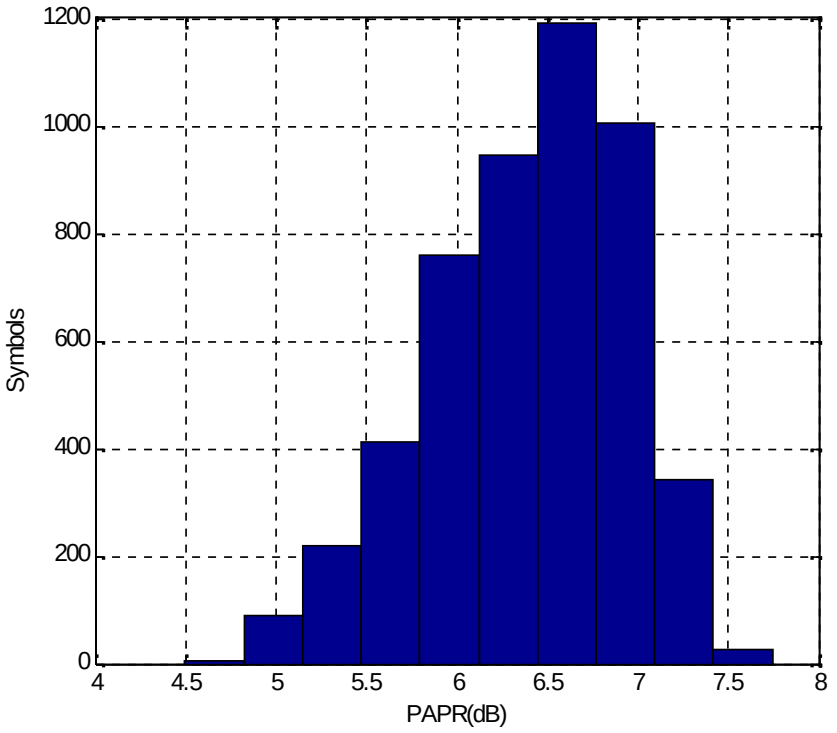

Figure 5.31: Histogram for PAPR after applying SLM with U=20

About 4.5 dB PAPR has been reduces by using 20 different phase sequence.

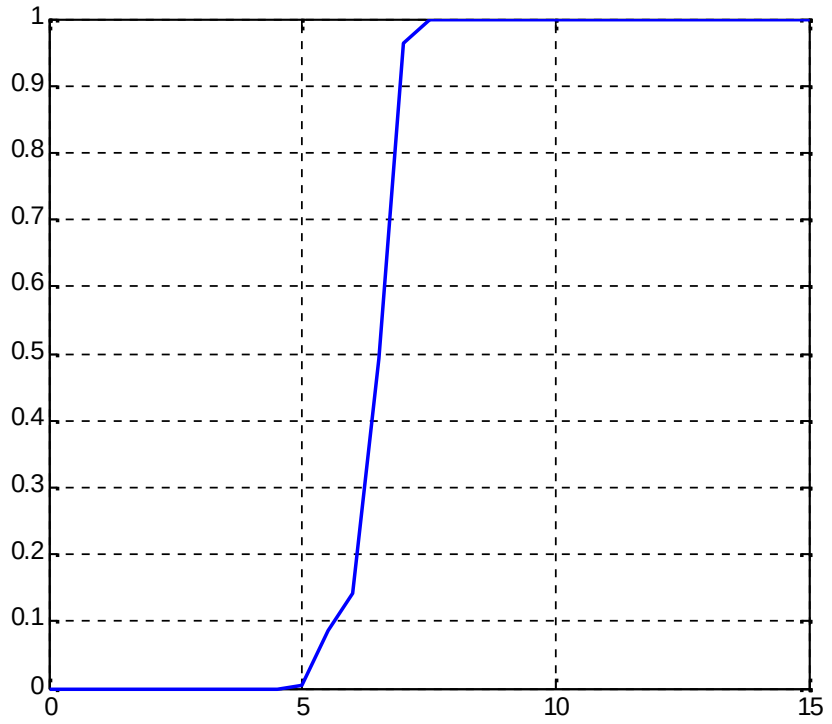

Figure 5.32: CCDF function for PAPR after applying SLM with U=30

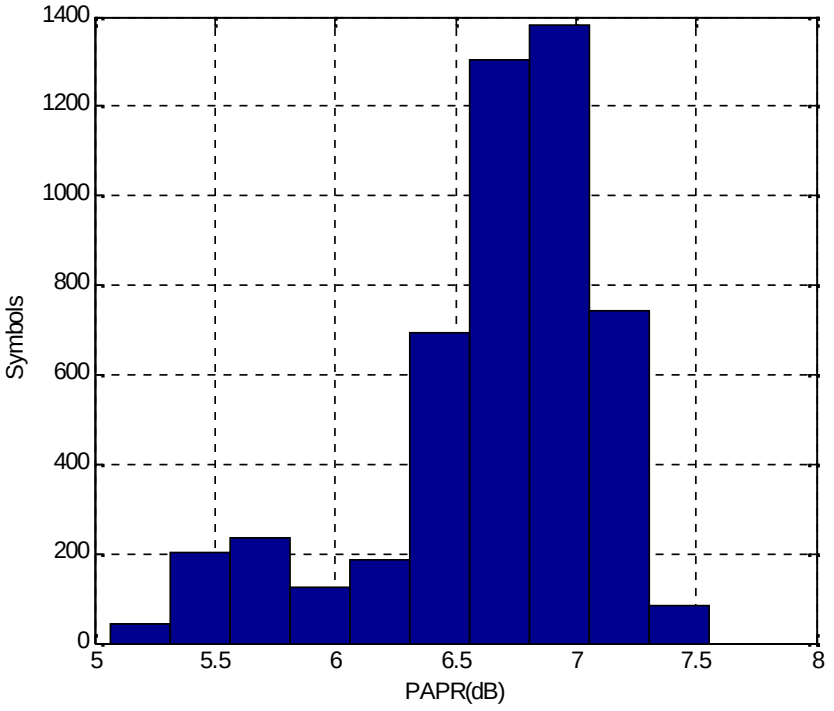

Figure 5.33: Histogram for PAPR after applying SLM with U=30

Around 5 dB PAPR has been reduces by using 30 different phase sequence.

Table 5.7: Summary of reduced PAPR and elapsed time

Number of Phase sequence(U)	Reduction in PAPR(dB)	Elapsed time(sec)
10	4	26.8790
20	4.5	34.4918
30	5	42.7599

From table 5.7 it has been observed that with minimum system latency significant amount of PAPR is reduced.

Chapter 6
CONCLUSION

Conclusion

In this thesis, the performance analysis of IEEE 802.11a has been carried out for different fading environments, Doppler shift, Cyclic Prefix (CP) and Forward Error Correction Code (FEC). It has been observed that as the data rate increases performance of IEEE 802.11a keeps on degrading. The loss of nearly 20 dB has been observed at BER 10^{-3} for 52 Mbps data rate as compare to 6 Mbps. It has also been observed, when there is no line of sight between receiver and transmitter (as in the case of Rayleigh fading channel) the performance of IEEE 802.11a degrades. Loss of 4 dB at BER 10^{-3} has been observed for Rayleigh fading channel, compared to Ricean fading channel. Outdoor condition where channel is supposed to follow Nakagami distribution, the performance of system further degrades. The Loss of 23 dB has been observed at BER 10^{-3} as compared to AWGN channel.

Further it has been observed, as the relative velocity between user and transmitter increases the degradation in the performance of IEEE 802.11a takes place due to Doppler shift. Here this fact is verified by simulating IEEE 802.11a for various Doppler shifts. Loss of 3.5 dB at BER 10^{-3} has been observed for 500 Hz Doppler compared to 100 Hz. It has also been observed that BER performance of IEEE 802.11a is improved with the use of CP and FEC. Finally the gain of 6 dB at BER 10^{-3} has been observed with CP of $0.8\mu sec$ and improvement of 1 dB has been observed with RS coding compared to CC in BER performance of IEEE 802.11a. Here the PAPR for IEEE 802.11a has been analysed and reduced using Selective Mapping technique (SLM).

REFERENCES

[1] R. O. Baldwin, N. J. Davis and S. F. Midkiff, *A Real Time Medium Access Control Protocol for Ad hoc Wireless Local Area Networks*, ACM New York, 1999, vol. 3.

[2] R. Prasad, *OFDM for Wireless Communications System*, 1st ed., Artech House, 2000.

[3] B. H. Walke, S. Mangold and L. Berlemann, *IEEE 802 Wireless Systems*, 1st ed. John Wiley & Sons, 2006.

[4] S. M. Schwartz "*Frequency Hopping Spread Spectrum (FHSS) vs. Direct Sequence Spread Spectrum (DSSS) in Broadband Wireless Access (BWA) and Wireless LAN (WLAN),*" Internet article: http://sorin-schwartz.com/white_papers/ f hvsds.pdf, 2010

[5] *Wireless LAN Medium Access Control (MAC) and Physical Layer (PHY) Specification*, IEEE Std. 802.11a, 1999.

[6] *Wireless LAN Medium Access Control (MAC) and Physical Layer (PHY) Specification*, IEEE Std. 802.11b, 1999.

[7] *Wireless LAN Medium Access Control (MAC) and Physical Layer (PHY) Specification*, IEEE Std. 802.11g, 2003.

[8] P. Latkoski, T. Janevski, and B. Popovski, "AP Placement and Channel Assignment in IEEE 802.11 WLAN," *in Proc. ETAI 2005*, pp. T-63-66.

[9] L. Wen, Z. Gao, G. Feng, D. Tang, and z. Ronghua; "Performance analysis of IEEE 802.11a in non saturation conditions," *in Proc IC-NIDC*, 2009, pp. 837-841.

[10] S.R. Mallipeddy and R.S Kshetrimayaum, "Impact of UWB interference on IEEE 802.11a," *Pro National Conference on Communication*, 2010, pp 1-5.

[11] Y. G. Li and G. L. Stuber, *Orthogonal frequency division multiplexing for wireless communications*, 1st ed. Springer Median, 2006.

[12] S. H. Han and J. H. Lee "An overview of peak to average power ratio reduction techniques for multicarrier transmission" *Wireless Communication*, IEEE vol. 12, pp. 56-65, Issue2 April 2005.

[13] J. Armstrong, "OFDM: From copper and wireless to optical," *Journal Of Lightwave Technology*, vol. 27, pp 189-204, 2009.

[14] G. Xiawen, B. Seungmin Baek and S. Park, "PAPR reduction of OFDM signal using an efficient SLM technique," *in Proc. 12 th ICACT*, 2010, vol.1, pp.324-328.

[15] R. H.Morelos, *The Art of Error Correcting Coding*, 2nd ed., Jhon Willey & Sons, 2002.

[16] B. Sklar, *Digital communication*, 2nd ed., Prentice Hall PTR, 1993.

[17] S. Haykin, *Communication Systems*, 4th ed., Wiley India, 2007.

[18] J.G. Proakis, *Digital Signal Processing*, 4th ed., Prason Prentic Hal, 2004.

[19] Web ProForum, "*OFDM for Mobile Data Communications*," Online Tutorial, Internet address: http://www.ice.org, 2010.

[20] M. Speth, "*OFDM Receivers for Broadband-Transmission*," Internet article: http:// www.ert.rwthaachen.de/projekte/Theory/OFDM/www_ofdm.html, 2010.

[21] A.M. Sayeed and B. Aazhang, Joint multipath doppler diversity in mobile wireless communications, *IEEE Transactions on Communication* ,vol. 47, pp. 123-132, Dec., 1999.

[22] J.C.I. Chuang, " The effect of time delay spread on portable radio channels with digital modulation," *IEEE J. Sel. Areas Commun*., pp. 879-889, 1987.

[23] Goldsmith, Andrea, *Wireless Communications*, 2nd Ed. Cambridge University Press, 2005.

[24] V. Valli, *"Optimum Recption in AWGN "* Internet article: http: //courses. ece. illinois.edu /ece461/handouts/notes7.pdf. 2010.

[25] N. L. Johnson, S. Kotz, and N. Balakrishnan, *Continuous Univariate Distributions*, 2nd ed. New York: Wiley, 1995, vol. 2.

[26] S. Bernard "Rayleigh Fading Channels in Mobile Digital Communication Systems part I : Characterization", *IEEE Communications Magazine*, pp 90–100, 1997.

[27] N. L. Johnson, S. Kotz, and N. Balakrishnan, *Continuous Univariate Distributions*, 2nd ed. New York: Wiley, 1995, vol. 2.

[28] A. Papoulis, *Probabilities, Random Variables, and Stochastic Processes*, 4th Ed. McGraw-Hill, 2002.

[29] A. Joshi, D.S. Saini, "Coded ODM in various multipath fading environments," *in Proc. 2nd ICCAE,*2010, vol.3, pp. 127-131.

[30] H. Kong and E. Shwedyk, "A hidden Markov model (HMM)-based MAP receiver for Nakagami fading channels," *in Proc. IEEE ISIT*, Whistler, BC, Canada, Sept. 17–22, 1995, pp. 210.

[31] M. Chandwani, A. Sighal, I. Naga, and V. Chakka "A Low Complexity SLM Technique for PAPR Reduction in OFDM Using Riemann Sequence and Thresholding of Power Amplifier," *in Proc. INDICON*, 2009, pp 1-4.